Manuscript Details

Title   In-situ trace metal (Cd, Pb, Cu) speciation along the Po River plume (Northern Adriatic Sea) using submersible systems.

Article type   Research Paper

Abstract

Information on the distribution and speciation of trace metals is of critical importance for our ability to interpret the links between the bioavailability and uptake of an element, and its biogeochemical cycle in coastal environments. Within the framework of the European Project "In-situ automated Monitoring of Trace metal speciation in Estuaries and Coastal zones in relation with the biogeochemical processes (IMTEC)", the chemical speciation of Cd, Pb and Cu was carried out along the Po River plume in the period 27 October – 2 November 2002. During the cruise five Voltammetric In-situ Profiling systems and one Multi Physical Chemical Profiler, as well as conventional voltammetric instruments, were successfully applied in order to evaluate the distribution of Cd, Pb and Cu between different fraction (free ion, dynamic, colloidal, dissolved and particulate fractions) and to assess the evolution of these fractions during the estuarine mixing and in the water column. Dynamic concentrations were 0.05-0.2 nmol L-1 Cd, 0.02-0.2 nmol L-1 Pb, and 0.15- 4.0 nmol L-1Cu. Cd was mainly present as dynamic fraction (40-100% of the dissolved Cd). High proportions of Pb (~70%) and Cu (~80%) were presents as colloids of probably biogenic origin. Principal components analysis reveals a strong influence of the Po River discharge on the spatial and vertical distributions of metal species. Almost all the metal fractions globally decreased following the salinity gradient. Metal concentrations are far below (at least one order of magnitude lower) the Environmental Quality Standard established by the Italian law. However, the Cu dynamic fraction showed concentrations likely to be toxic to sensitive phytoplankton community and to have negative effects on larva development of coastal macroinvertebrate species (toxicity data extracted from literature).

Taxonomy   Marine Pollution, Metal Biogeochemistry, Environmental Chemistry Substances, Marine Chemistry, Environmental Science

Corresponding Author   Cristina Truzzi

Corresponding Author's Institution   Departement of Life and Environmental Sciences, Università Politecnica delle Marche

Order of Authors   Silvia Illuminati, Anna Annibaldi, Cristina Truzzi, Marylou Tercier-Waeber, Charlotte Braungardt, Eric Achterberg, David Turner, mauro marini, Tiziana Romagnoli, Cecilia Maria Totti, Flavio Graziottin, Jacques Buffle, Giuseppe Scarponi

Suggested reviewers   Roko Andricevic, Matthieu Waeles, Sabina Susmel, Clara Turetta, Ana-Marija Cindric

Submission Files Included in this PDF

File Name [File Type]

CoverLetter.docx [Cover Letter]

Highlights.docx [Highlights]

Illuminati_Me-Speci_AS.docx [Manuscript File]

Fig.1.docx [Figure]

Fig.2.docx [Figure]

Fig.3.docx [Figure]

Fig.4.docx [Figure]

Fig.5.docx [Figure]

Fig.6.docx [Figure]

Fig.7.docx [Figure]

Fig.8.docx [Figure]

Fig.9.docx [Figure]

SupportingInformation.docx [Figure]

Fig.S1.docx [Figure]

To view all the submission files, including those not included in the PDF, click on the manuscript title on your EVISE Homepage, then click 'Download zip file'.

Dear Sirs,

I enclose a manuscript entitled

"In-situ trace metal (Cd, Pb, Cu) speciation along the Po River plume (Northern Adriatic Sea) using submersible systems"

by

Silvia Illuminati, Anna Annibaldi, Cristina Truzzi, Mary-Lou Tercier-Waeber, Stéphane Nöel, Charlotte B. Braungardt, Eric P. Achterberg, Kate A. Howell, David Turner, Mauro Marini, Tiziana Romagnoli, Cecilia Totti, Fabio Confalonieri, Flavio Graziottin, Jacques Buffle, Giuseppe Scarponi

to be considered for publication as Research Paper in "Marine Chemistry".

The manuscript describes and discusses the results on the chemical speciation of Cd, Pb and Cu carried out along the Po River plume, Adriatic Sea

It presents some interesting news: (1) the application of voltammetric sensors (Voltammetric In-situ Profiler and Multi Physico-Chemical Profiler) allowing the evaluation in-situ of Cd, Pb and Cu specie distribution; (2) the assessment of the evolution of metal fractions during the estuarine mixing and in the water column; (3) the multivariate statistical analysis applied to the overall dataset revealed a strong influence of the Po River discharge on the spatial and vertical distributions of metal species; (4) the metal concentrations are one order of magnitude lower than the Environmental Quality Standard established by the Italian law; (5) the Cu dynamic fraction showed concentrations likely to be toxic to sensitive phytoplankton community and to have negative effects on larva development of coastal macroinvertebrate species.

Please, note that two authors (Fabio Confalonieri and Flavio Graziottin) have the same e-mail addresses, the only available. One of the authors, Kate A. Howell, is dead. Anyway, we would like to include her name in the author's list, in memory of her strong contribution to the project and…of her smile.

Thanking you in advance for your attention,
Yours sincerely,

Dr. Silvia Illuminati
Polytechnic University of Marche – Ancona,
Department of Life and Environmental Sciences,
Via Brecce Bianche, 60131, Ancona, Italy
E-mail: s.illuminati@univpm.it

Research Highlights

- First speciation study on trace metals in the Adriatic Sea
- In-situ speciation by submersible, reliable voltammetric sensors
- Metal species distribution mainly affected by Po River outflow
- Metal dynamic concentrations below legal limits
- Cu dynamic concentrations toxic to sensitive phytoplankton

In-situ trace metal (Cd, Pb, Cu) speciation along the Po River plume (Northern Adriatic Sea) using submersible systems.

Silvia Illuminati[a][1], Anna Annibaldi[a][1], Cristina Truzzi*[a], Mary-Lou Tercier-Waeber[b], Stéphane Nöel[b], Charlotte B. Braungardt[c], Eric P. Achterberg[d], Kate A. Howell[c,e], David Turner[f], Mauro Marini[g], Tiziana Romagnoli[a], Cecilia Totti[a], Fabio Confalonieri[h], Flavio Graziottin[h], Jacques Buffle[b], Giuseppe Scarponi[a]

[a]Department of Life and Environmental Sciences, Università Politecnica delle Marche, Italy
[b]CABE, Department of Inorganic and Analytical Chemistry, University of Geneva, Switzerland
[c]School of Earth, Ocean and Environmental, University of Plymouth, UK
[d]GEOMAR, Helmholtz Centre for Ocean Research Kiel, Germany
[e]Nanotecture Ltd. Epsilon House, Southampton Science Park, UK
[f]Department of Marine Sciences, University of Gothenburg, Sweden
[g]Institute of Marine Science, National Research Council (CNR), Ancona, Italy
[h]Idronaut Srl, Brugherio (MI), Italy

[1]Both authors contributed equally to this manuscript

Contact information for Corresponding Author
*Cristina Truzzi, Department of Life and Environment Sciences, Università Politecnica delle Marche, Via Brecce Bianche, 60131 Ancona, Italy. Phone: +390712204981 Fax: +390712204650. E-mail: c.truzzi@univpm.it

Abstract

Information on the distribution and speciation of trace metals is of critical importance for our ability to interpret the links between the bioavailability and uptake of an element, and its biogeochemical cycle in coastal environments. Within the framework of the European Project "In-situ automated Monitoring of Trace metal speciation in Estuaries and Coastal zones in relation with the biogeochemical processes (IMTEC)", the chemical speciation of Cd, Pb and Cu was carried out along the Po River plume in the period 27 October – 2 November 2002. During the cruise five Voltammetric In-situ Profiling systems and one Multi Physical Chemical Profiler, as well as conventional voltammetric instruments, were successfully applied in order to evaluate the distribution of Cd, Pb and Cu between different fraction (free ion, dynamic, colloidal, dissolved and particulate fractions) and to assess the evolution of these fractions during the estuarine mixing and in the water column. Dynamic concentrations were 0.05-0.2 nmol L^{-1} Cd, 0.02-0.2 nmol L^{-1} Pb, and 0.15- 4.0 nmol L^{-1}Cu. Cd was mainly present as dynamic fraction (40-100% of the dissolved Cd). High proportions of Pb (~70%) and Cu (~80%) were presents as colloids of probably biogenic origin. Principal components analysis reveals a strong influence of the Po River discharge on the spatial and vertical distributions of metal species. Almost all the metal fractions globally decreased following the salinity gradient. Metal concentrations are far below (at least one order of magnitude lower) the Environmental Quality Standard established by the Italian law. However, the Cu dynamic fraction showed concentrations

38   likely to be toxic to sensitive phytoplankton community and to have negative effects on larva development of coastal

39   macroinvertebrate species (toxicity data extracted from literature).

40

41

42   **Keywords**

43   Metals; Speciation; Estuary; Voltammetry

44

45   **1. Introduction**

46   The Adriatic Sea is a semi-enclosed shelf basin located in the northeast part of the Mediterranean Sea and it is strongly

47   influenced by several riverine inputs. In its northern sub-basin, the freshwater plume of the Po River plays a fundamental

48   role in driving the coastal dynamics and the physical and biogeochemical processes of the whole basin. Crossing the

49   entire northern part of the Italian country, which is one of the most industrialized areas in Europe, the Po river discharges

50   in the Adriatic Sea a remarkable load of pollutants, which in turns affect the Italian coasts even to approximately the city

51   of Ancona (following the prevailing southward marine currents).

52   The Northern Adriatic Sea has been intensely investigated, studying the physical structure of the water column, as

53   well as the circulation patterns (Russo and Artegiani, 1996; Falcieri et al., 2014), the plankton community (Totti et al.,

54   2005; Cabrini et al., 2012; Godrijan et al., 2013), the nutrient (Boldrin et al., 2005; Grilli et al., 2013) and trace element

55   distribution in seawater (Annibaldi et al., 2009, 2011, 2015; Cindrić et al., 2015; Tankere and Statham, 1996; Zago et al.,

56   2000, 2002).

57   Nowadays, following the enactment of specific EU Directives, there is a growing need to control the quality of coastal

58   waters, which are affected by several anthropogenic activities (building of infrastructure for human settlement, habitat

59   modification, tourism, transport by sea and disposal of industrial and domestic effluents). Combined efforts are requested

60   to develop monitoring and assessment programs in order to survey and guarantee a good chemical and ecological status

61   of the coastal ecosystems, including heavy metals. Heavy metals are ubiquitous in the environment and their

62   concentrations are increased with respect to natural pre-industrial values due to anthropogenic activities, which have

63   modified at the same time, metal biogeochemical cycles on a regional and global scale (Sadiq, 1992). It is well known

64   that the toxicity, bioavailability and mobility of trace metals in seawater depend on their speciation rather than on the only

65   total concentration (Allen and Hansen, 1996). Dissolved trace metals in seawater can exist in different chemical species

66   (forms), such as free hydrated ions, organic and inorganic complexes. The study of the metal species distribution in

67   seawater gives insights on their cycles, as each metal species is characterized by different reactivity and different

68   interactions with organisms. Free hydrated ions are the most reactive and highly bioavailable, but their reactivity, as well

69 as their toxicity can be greatly modified by the presence of organic and inorganic compounds. Thus, to better understand

70 the biogeochemical cycle of a trace metal and its overall mobility in the water column, it is essential to identify and

71 quantify the various species that make up its total concentration.

72   Across much of the world, regulatory limit values (e.g., Environmental Quality Standards in the EU, Water Quality

73 Criteria in the US, Australia, Canada, etc.) for metals in water bodies do not take metal speciation into account. They are

74 mainly based on dissolved metal, since this fraction more closely approximates the bioavailable fraction of the metal in

75 the water column. Recently, thanks to a major refinement in the scientific understanding of the behavior, fate and

76 toxicology of metals in the environment, and to a series of statutory and voluntary risk assessments performed under the

77 existing regulations on pollutant monitoring program, several public administrations started to implement the in-force

78 water quality assessments by introducing a speciation-based approach. The revised Priority Substances Daughter

79 Directive, 2013/39/EU (2013) includes now annual average Environmental Quality Standards (EQS) for nickel and lead

80 in the freshwater environment that refer to bioavailable concentrations. These bioavailable EQS are based on Biotic

81 Ligand Models (BLM), but, at the time of the development of the latest draft of the Water Framework Directive, there

82 was no validated and accepted BLM for some metals, therefore complimentary availability-based approaches were

83 adopted to define the EQS bioavailable. For example, the EQS for lead are based on the availability correction for the

84 dissolved organic carbon (SCHEER-EC, 2017).

85   Very few studies reported chemical speciation of trace metals in the Adriatic Sea, the most of them dealing with the

86 horizontal and vertical partitioning between dissolved and particulate phases (Tankere and Statham, 1996; Tankere et al.,

87 2000; Zago et al., 2000, 2002; Annibaldi et al., 2011, 2015; Cindrić et al., 2015). Some authors (Scarponi et al., 1995,

88 1998), through voltammetric titration, studied the distribution of dissolved trace metals between the free fraction (mainly

89 ionic and inorganic complexed metal) and bound fraction (organically complexed metal), as well as the content of ligands

90 complexing metal and the related conditional stability constants.

91   Within the framework of the European Project "In-situ automated Monitoring of Trace metal speciation in Estuaries

92 and Coastal zones in relation with the biogeochemical processes (IMTEC)", several studies on metal speciation were

93 carried out in different European coastal areas by the partners of the project (University of Geneva, University of

94 Göteborg, University of Plymouth, University of Ancona, University of Neuchatel).

95   This paper focuses on the chemical speciation of Cd, Pb and Cu along the Po River plume, which is particularly

96 significant for the study of physical, hydrological and biological processes that affect trace metal contents and

97 distributions during the estuarine mixing, and for the better understanding of the behaviour and fate of the different metal

98 species. The speciation studies were carried out by applying submersible voltammetric probes, that were developed and

99 tested within the IMTEC project for the trace element monitoring in natural environments.

100   The Voltammetric In-situ Profiling (VIP) probe is the first commercially available instrument (Idronaut, Italy)

101   developed by Tercier and co-workers (Tercier et al., 1998) that combines trace metal speciation analysis of high sensitivity

102   and resolution with automated in-situ operation and options for remote deployment. The VIP allows the long-term, real-

103   time and simultaneous determination of a fraction of the conventional total dissolved trace metal, the so-called "dynamic

104   fraction", of several trace metals, directly in the water column, with no or minimum pretreatments. The dynamic fraction

105   is defined as the sum of the free metal ions and the sufficiently labile (high dissociation rate) and mobile (high diffusion

106   rate) inorganic and organic complexes of a few nanometers in size (Buffle and Tercier-Waeber, 2005). This metal fraction

107   is of great importance, as it represents the concentration of metals potentially bioavailable, i.e. the dynamic metal

108   complexes may dissociate within the time it takes to diffuse from the bulk medium to an organism's cell surface receptor

109   site, and hence be readily available (Buffle and Tercier-Waeber, 2005). This is possible due to a specifically designed

110   gel-integrated microelectrode (GIME) that consists of an array of 100 interconnected Ir-based micro-disc electrodes,

111   coated with an antifouling gel membrane of 300 μm thickness (for more details see Belmont-Hebert et al., 1998). The

112   non-dynamic fraction, comprising metals associated with colloidal material cannot be determined by the VIP system

113   (Buffle and Tercier-Waeber, 2005; Braungardt et al., 2011). Generally, colloids are micro particles and macromolecules

114   in the size range of 1 nm to 1 μm with 1nm $\cong$ 1 kDa for globular macromolecules. They can have an inorganic (clays,

115   metal oxides, metal hydroxides, and metal carbonates) or organic (detrital matter, e.g. fulvic and humic acids, and living

116   organism, such as algae, bacteria, virus) nature. Because of their high capacity of adsorbing considerable amounts of trace

117   metals, due to a large specific area and, consequently, of a high number of active sites (Vignati and Dominik, 2003),

118   colloids play a critical role in controlling metal speciation and the cycling of many elements in natural waters. The

119   colloidal fraction of metals can be deduced from the difference between the total dissolved metal concentration and the

120   dynamic concentration, according to Braungardt et al., 2011. A more sophisticated system, called Multi Physical

121   Chemical Profiler (MPCP), has also been developed to extend the capability of the VIP to *in situ* monitoring of trace

122   metal speciation (Tercier-Waeber et al., 2005). The MPCP allows the simultaneous *in situ*, autonomous monitoring and

123   profiling (down to 150 m) of three major metal fractions: i) the free metal ion concentration, (i.e. the species related to

124   biological uptake) by means of a particular GIME sensor, the complexing gel integrated micro-electrode (CGIME), which

125   is covered by a thin 3.5 μm layer of a Microchelex chelating resin which in turns is covered by a thick 300 μm antifouling

126   agarose gel (details of CGIME measurement principles and preparation in Noel et al., 2006); ii) the dynamic metal species

127   by a GIME sensor; and iii) the total acid-extractable metal concentration by means of a GIME sensor coupled to a

128   submersible flow-injection analysis (FIA) system (Tercier-Waeber et al., 2005, 2008). The MPCP is coupled with a CTD

129   probe for the measurement of the master variables (pressure, temperature, pH, oxygen, conductivity, salinity, redox

130   potential, turbidity and chlorophyll-a). Both the VIP and the MPCP have been successfully applied in several

4

environments, i.e. freshwater (Tercier-Waeber et al., 1998, 2002; Tercier-Waeber and Buffle, 2000), groundwater, fjord water (Tercier-Waeber et al., 1999), macro-tidal estuaries (Tercier-Waeber et al., 2005; Braungardt et al., 2009) and coastal marine waters (Tercier-Waeber et al., 1999, 2005; Howell et al., 2003; Braungardt et al., 2009).

In the autumn 2002 a joint oceanographic cruise was carried out along the Po river plume in order i) to evaluate the metal distribution between different fractions (free ion, dynamic, colloidal, dissolved and particulate fractions) and their relationship with the total content; ii) to assess the evolution of the different metal fractions during the estuarine mixing and in the water column; and iii) to evaluate the effect of the hydrological characteristics of the water column, as well as of phytoplankton, on metal speciation. Moreover, preliminary tests of the CGIME sensor on discrete samples were also carried out. As the validation of new technique measurements in complex media is not straightforward, hollow fiber permeation liquid membrane (HF-PLM) coupled to an inductively coupled plasma mass spectrometer (ICP-MS) were used in parallel to CGIME measurements for comparison purposes. This technique allows the measurements of free metal ions and some lipophilic contribution (Parthasarathy et al., 1997).

2. Materials and Methods

2.1. Laboratory, apparatus and reagents

A clean room laboratory ISO 14644-1 Class 6 (or US Fed. Std. 209e Class 1000), with areas at ISO Class 5 (or US F. S. 209e Class 100) under laminar flow cabinets, was available for trace metal clean working conditions. A portable laminar flow hood was available on board for sample treatments and analyses carried out on-site. Clean room garments, masks and gloves were worn by the personnel, who strictly followed clean room procedures during the most critical analytical steps.

Seawater sampling bottles were 8-L and 10-L GO-FLO from General Oceanics (Florida, USA). CTD probes, mod. Ocean Seven 316 CTD and Ocean Seven 301 were from Idronaut (Milan, Italy). The Handheld Salinity, Conductivity and Temperature System, Mod. 30, was from YSI (Yellow Springs, OH, USA). The Portable Turbidimeter Model 966 was from Orbeco-Hellige (New York, USA).

Filtration systems were the Sulfoflo from Nalgene (Rochester, New York) equipped with 0.45 μm pore size membrane filters (cellulose mixed esters ⌀ 47 mm, Schleicher & Schuell, Dassel, Germany) and the glassware apparatus with pre-weighted filter membranes. The UV digestion apparatus was the Mod. 705 UV-digester from Metrohm, (Herisau, Switzerland), equipped with twelve 12-mL quartz vessels and a 500 W mercury lamp. The Mod. 290A pH-meter, equipped with an Orion epoxy pH electrode Sure-Flow (Mod. 9165BN) was from Orion (Beverly, MA, USA). For

5

phytoplankton analyses, the inverted microscope, Mod. Axiovert 135, and the epifluorescence microscope Mod. Axioplan were from Zeiss (Milan, Italy). For nutrients, the Technicon Autoanalyzer Traacs 800 system was from Seal Analytical (Norderstedt, Germany). Plastic containers were of low-density polyethylene material (Kartell, Italy). The polyethylene bottles, the quartz vessels, the sampling equipment, the filtration apparatus and all other plastic containers were decontaminated following the procedure reported elsewhere (Illuminati et al., 2015). Details of the decontamination procedure are briefly described in Supporting Information, text S1.

The instrumentation for metal speciation consisted of (i) two Metrohm (Herisau, Switzerland) 746 VA Trace Analyser and two 747 VA Stand, each one equipped with a Teflon PFA (perfluoroalkoxy copolymer) cell and a three-electrode system, which includes an epoxy-impregnated graphite rotating disk working electrode (as a support for the thin mercury film electrode, TMFE), an Ag/AgCl, KCl 3 mol L^{-1} reference electrode (to which all potentials are referred throughout) and a glassy carbon rod counter electrode; (ii) five Voltammetric *In-situ* Profiling (VIP) systems (Idronaut, Italy), equipped each one with a pressure compensated mini flow-through Plexiglas voltammetric cell comprising a Gel Integrated Mercury-plated Microelectrode (GIME sensor), an Ag/AgCl, KCl saturated gel reference electrode and a built-in platinum ring auxiliary electrode; (iii) one Multi Physical-Chemical Profiler (MPCP) equipped with two VIP systems and one submersible Flow-Injection Analysis (FIA) system; (iv) one Amel potentiostat equipped with a Metrohm cell based on a three-electrode configuration which includes a CGIME sensor, an Ag/AgCl/KCl$_{(satured)}$ reference electrode and a platinum rod counter electrode; and (v) one Hollow Fiber Permeation Liquid Membrane (HF-PLM) device coupled to an ICP-MS. Transferpette variable volume micropipettes from Brand (Wertheim, Germany) and neutral tips were used.

Ultrapure water was Milli-Q from Millipore (Bedford, MA, USA). Ultrapure HCl (34.5%), HNO_3 (70%), H_2O_2 (ca. 30%), and superpure $HClO_4$ (65%) were from Romil (Cambridge, England; UpA grade). Superpure KCl, $Hg(CH_3COO)_2$, hexadistilled mercury, KSCN and $NaNO_3$ were from Merck (Darmstadt, Germany). 1.5% LGL agarose gel was from Biofinex (Neuchâtel, Switzerland). Atomic absorption standards of Cd (II), Pb (II) and Cu (II) were from Carlo Erba (Milan, Italy). Research-grade nitrogen, purity $\geq$ 99.999%, was from Sol (Monza, Italy). The estuarine water reference material SLEW-3, the nearshore-seawater reference material CASS-4, the seawater reference material NASS-5 for trace metals were from the National Research Council of Canada.

2.2. Study area

The Adriatic Sea can be divided in three regional basins (North, Central and South), differing in bathymetry, hydrology, morphology and biogeochemical features (Russo and Artegiani, 1996). The northern basin, with a width of about 75 nautical miles and a mean depth of 30 m (maximum depth about 70 m), is the shallower part of the Adriatic

193 epicontinental shelf. It is characterized by large inputs of freshwaters from several rivers mainly concentrated along the

194 northern and the north-western coast of Italy. The Po River is the Italy's largest river (with a length of 673 km and drainage

195 basin of 71,000 km^2) and it flows through one of the most industrialized regions of the country. It has an annual outflow

196 rate of 1500 – 1700 m^3 s^{-1}, accounting for about one third of the total riverine freshwater input into the Adriatic Sea

197 (Marini et al., 2010). Discharge peaks of about 2000 m^3 s^{-1} are generally observed in spring (May-June) following the

198 snow melting, and in autumn (October-November) when intense rainfall contributes to Po river discharge (Boldrin et al.,

199 2005; Marini et al., 2008).

200   The oceanographic cruise in the Northern Adriatic Sea was carried out on board of *G. Dallaporta* vessel (CNR,

201 Ancona, Italy) from October 27th to November 4th 2002, along a transect of six stations from the Po mouth toward the

202 open sea, in direction East – South East (Fig. 1). About five stations were located in the plume while the remaining one

203 was outside. For a better representation of data, the study area was divided into three different zones. According to Falcieri

204 et al., 2014 (who carried out a 8-year simulation of the Po plume mean spatial variability based on data of temperature,

205 salinity and currents collected during September 2002 as initial conditions), we marked the limit for the front between the

206 plume and the sea water at the surface salinity of ~36. Here, we called "pro-delta area" the first segment of the transect,

207 which was 10-km away from the Po mouth. This segment was characterized by high fluctuations of salinity (from ~18 to

208 ~29) and it included Stns. 1 and 2. The second segment, called "frontal area", extended from 10 km to ~40 km from the

209 Po mouth. It was characterized by more stable salinity values (from ~33 to ~36) and it includes Stns. from 3 to 5. Finally,

210 the third segment was called "marine area", which included the Stn. 6 and it was characterized by marine water masses

211 not influenced by the Po River (Fig. 1). To be noted that Stn. 5 had surface salinity around 36 and it should be part of the

212 marine area, nevertheless, it was included in the second segment of the transect, because at this station most of all the

213 variables studied had a behaviour comparable to the frontal area instead of the marine one.

214

215 2.3. Sample collection and treatments

216   During the oceanographic cruise, two kinds of speciation were carried out. The first type dealt with the *in situ*-based

217 speciation using several VIPs and one MPCP (equipped with two VIPs and one GIME-FIA system) for the determination

218 of the dynamic (Me$_{dyn}$) and the total acid-extractable (Me$_{ac.extr}$) fractions of Cd, Pb and Cu in the water column. The

219 second type regarded the on board/laboratory-based speciation carried out on discrete samples collected at the same depths

220 of the VIP and MPCP deployment, by means of the conventional Metrohm instrumentations for the total and dissolved

221 metal concentration measurements. Discrete samples were also collected for immediate on-board analysis of both

222 dynamic and total extractable fractions on surface samples, since the VIP and MPCP probes, due to their manufacture

223 characteristics, cannot be used in depths < 1 m (Tercier et al., 1998; Tercier-Waeber et al., 2005).

224　　　Surface samples were collected manually in polyethylene bottles by a rubber dinghy at ~1 km from the oceanographic

225　　vessel. Immediately after collection, the samples were divided in various aliquots that were subjected to different

226　　treatments in order to obtain the different metal fractions. The first was acidified (raw sample) with ultrapure HCl (2:1000,

227　　pH ~2) for the determination of the total metal concentration (Me_{tot}). An aliquot was filtrated through 0.45-μm pore-size

228　　membrane filter and then acidified with ultrapure HCl (2:1000, pH ~2) for the determination of the dissolved metal

229　　contents (Me_{diss}). Before analysis, all the acidified samples (both raw and filtered) were subjected to photo-oxidative

230　　digestion, by UV irradiation for 12 h after the addition of 1:1000 ultrapure H_2O_2, in order to destroy organic matter, to

231　　leach bound metals, and to avoid possible adverse effect on the voltammetric determination (Kolb et al., 1992). Total

232　　particulate metal concentration (Me_{part}) was obtained by difference between the total and the dissolved concentrations,

233　　while the metal concentration in the colloidal fraction (Me_{coll}) was computed as difference between the dynamic and the

234　　total dissolved concentration.

235　　　Aliquots of seawater samples were acidified with ultrapure HCl (2:1000, pH ~2) and then analysed on board without

236　　UV digestion for the determination of the total HCl-extractable metal fraction to compare it with that measured by the

237　　GIME-FIA system. Other seawater aliquots were used, without any treatments, for the determination on board of the free

238　　metal ion concentration (Me_{free}) using both CGIME sensor and the PLM technique. Finally, other seawater aliquots were

239　　used to measure turbidity, DOC and nutrients.

240

241　　2.4. Metal speciation methodology

242　　　Cd, Pb and Cu were determined simultaneously using the square-wave anodic stripping voltammetry (SWASV) that

243　　was implemented both on conventional laboratory instrumentation and on voltammetric probes for the in-situ

244　　measurements.

245

246　　2.4.1. *In situ*-based speciation

247　　　The dynamic fraction and the in-situ total acid extractable concentration of Cd, Pb and Cu were determined by using

248　　the VIP and the MPCP systems.

249

250　　*VIP system*. The voltammetric determination of the metal dynamic fractions required the initial Hg deposition on the Ir

251　　substrates of the GIME sensors, by applying a constant potential of −400 mV for 6 min in a N_2 de-oxygenated solution

252　　of $Hg(CH_3COO)_2$ (5 mmol L^{-1}) and $HClO_4$ (10^{-2} mol L^{-1}) (Belmont-Hebert et al., 1998). The Hg film remained in place

253　　for the entire period of the oceanographic cruise. The Hg film was removed by scanning the potential from −300 mV to

254　　+300 mV at 5 mV s^{-1} in a N_2 de-oxygenated solution of KSCN (1 mol L^{-1}). The voltammetric analyses were performed

8

255   in successive steps: (i) sample pumping through the cell for 3 min at 7 mL min^{-1}; (ii) equilibration of the agarose gel with

256   the sample for 5-6 min; (iii) SWASV measurements inside the gel, using the background subtraction technique (Belmont-

257   Hebert et al., 1998), and the following instrumental parameters: deposition potential, E_{dep} = −1100 mV; deposition time,

258   t_{dep} = 10 to 45 min (as a function of the metal concentrations); final potential, E_{fin} = −50 mV in sea water, +120 mV in de-

259   oxygenated NaNO$_3$ (0.1 mol L^{-1}) electrolyte during laboratory calibration; equilibration potential, E_{equil} = −1100 mV;

260   equilibration time, t_{equil} = 20 s; pre-cleaning potential, E_{precl} = −50 mV (in sea water), +120 mV (in NaNO$_3$); pre-cleaning

261   time, t_{precl} = 20 s; pulse amplitude, E_{SW} = 25 mV; step amplitude, ΔE_{step} = 8 mV; frequency, f = 200 Hz.

262   *MPCP system*. The three-channel system of the MPCP constituted of two GIME sensors for the determination of the

263   dynamic fractions (instrumental parameters as for other VIP probes), and a GIME-FIA system for the determination of

264   the in-situ total extractable metal concentrations. The latter were measured in three steps: (1) on-line pre-treatments based

265   on ligand exchanges followed by acidification and heating of the sample to release trace metals complexed and/or

266   adsorbed; (2) equilibration of the sensor agarose gel with the pre-treated sample; (3) SWASV measurements of total

267   extractable metal concentration (Tercier-Waeber et al., 2005). The conditions used for the sample pre-treatment were as

268   follows: ligand stock solution = 150 µmol L^{-1} of triethylenetetramine (TRIEN); acid stock solution = 3.3 × 10^{-2} mol L^{-1}

269   superpure NaNO$_3$; sample, ligand and acid flow-rates = 4.2 mL min^{-1}, 2.4 mL min^{-1} and 3.2 mL min^{-1} corresponding to

270   dilution factors of 2.3, 4.1, and 3.1 for the sample, ligand and acid, respectively (i.e. reagents concentration in the pre-

271   treated samples; 36.6 µmol L^{-1} TRIEN, 9.7 × 10^{-3} mol L^{-1} superpure NaNO$_3$); equilibration time sample+ligand = 2 min;

272   equilibration time sample+ligand+acid at 50 °C = 2 min. The SWASV parameters used were as follows: equilibration

273   time of the agarose gel with the pre-treated sample = 6 min; E_{dep} = −950 mV; t_{dep} = 5 to 15 min (as a function of the metal

274   concentrations, during *in situ* deployments); E_{fin} = −50 mV in sea water or +120 mV in laboratory calibration in superpure

275   NaNO$_3$; E_{equil} = −1100 mV; t_{equil} = 20 s; E_{precl} = −50 mV to +120 mV; t_{precl} = 20 s; E_{SW} = 25 mV; ΔE_{step} = 8 mV; f = 200

276   Hz.

277

278   The quantification of both the dynamic and the total extractable concentration was obtained using the calibration curve

279   method, in N$_2$ degassed 0.1 mol L^{-1} NaNO$_3$ standard solutions spiked with various concentrations of Cd, Pb and Cu. The

280   resulting slopes were normalized (Tercier-Waeber et al., 1999) after: (1) smoothing of the currents (using Golay-Savitzky

281   moving average); (2) subtraction of the background current from the current signal; (3) peak height quantification; and,

282   where necessary, (4) temperature effect correction on peak current measured *in situ* (Tercier-Waeber et al., 1998; Howell

283   et al., 2003). The calibration procedure was performed before and at end of the oceanographic campaign, while the validity

284   of slopes was tested during the cruise, on board, by analysing a N$_2$-degassed standard solution previously used in the

285   calibration curve procedure.

287   2.4.2. On board/laboratory-based speciation

288   *Metrohm system*. Total and the dissolved metal fractions were determined in land-based laboratory (within 1-3 months

289   after the sample collection) by conventional Metrohm instrumentation. The procedure involved the pouring of a 10-mL

290   UV-digested sample aliquot into a pre-cleaned voltammetric cell, where the thin mercury film electrode (TMFE) was

291   already prepared and tested (Annibaldi et al., 2007; Illuminati et al., 2013, 2015). The $Hg(NO_3)_2$ solution (2.5×10^{-2} mol

292   L^{-1}) for the TMFE was obtained by oxidation of hexadistilled mercury with ultrapure nitric acid. The voltammetric

293   analyses were carried out in the background subtraction technique, using the following instrumental parameters:

294   E_{dep} = −975 mV; t_{dep} = 3 to 10 min (as a function of the metal concentrations, during *in situ* deployments); E_{fin} = 0 mV;

295   E_{equil} = −975 mV; t_{equil} = 7.5s; E_{precl} = −50 mV; t_{precl} = 5 min; E_{SW} = 25 mV; f = 100 Hz; ΔE_{step} = 8 mV; t_{step} = 150 ms.

296   Two-three replicates were carried out with the sample in the cell, after which quantification was obtained using the

297   multiple standard addition method.

298   *CGIME sensor*. Preliminary tests for the determination of the free metal ion concentration with the complexing gel

299   integrated microelectrode (CGIME) were carried out on discrete samples on board, by using a standard Amel potentiostat

300   with a three-electrode Metrohm cell. First, mercury films were deposited on CGIME sensor, by applying a constant

301   potential of −400 mV for 8 min in a N_2 de-oxygenated 5 mmol L^{-1} $Hg(CH_3COO)_2$ and 10^{-1} mol L^{-1} $HClO_4$ solution

302   (Tercier et al., 1995). Removal of the mercury film was carried out with the same procedure used for GIME sensors (see

303   above). The measurement of free metal ion concentrations was performed in two steps: (1) equilibration of the sensor

304   with the sample to accumulate trace metals on the Microchelex resin in proportion to free metal ion concentrations in

305   seawater; (2) transfer of the CGIME sensor in a glass cell filled with an acid solution (0.1 mol L^{-1} $NaNO_3$ + 0.1 mol L^{-1}

306   superpure HNO_3). Here, the accumulated metals were released by acid and then, immediately detected by SWASV using

307   the following instrumental parameters (Noel et al., 2006; Tercier-Waeber et al., 2005): accumulation time = 1 to 2 h, with

308   a renewal of the sample in the cell every 15 min; E_{dep} = −900 mV; t_{dep} = 10 to 30 min; E_{fin} = +100 mV; E_{SW} = 25 mV;

309   ΔE_{step} = 8 mV; f = 50 Hz.

310   *HF-PLM technique*. Hollow Fiber Permeation Liquid Membrane (HF-PLM) coupled to ICP-MS detection was used for

311   laboratory measurements performed in some discrete samples for comparison purposes with the CGIME measurements

312   of the free metal ion concentrations. The analytical procedure used for the HF-PLM preparation and measurements

313   included different steps (Parthasarathy et al., 1997, 2001): (1) preparation of the hollow fiber which was a loosely, coil,

314   single polypropylene hollow fiber with an inner diameter of 600 µm; (2) impregnating of hollow fiber with the organic

315   metal carrier (0.1 mol L^{-1} 1,10-didecyl diaza 18-crown-6 and 0.1 mol L^{-1} lauric acid dissolved in a mixture of

316   phenylhexane and toluene); (3) metal separation and pre-concentration, in which the impregnated hollow fiber membrane

317   was immersed in the sample solution placed in a plastic beaker and held vertical by means of a clamp; (4) filling of the

318   lumen side of the hollow fiber with 5×10^{-4} mol L^{-1} CDTA (trans-cyclohexanediamine tetra-acetic acid) strip solution

319   adjusted to pH 6.4 with NaOH; (5) collection of the strip solution by pushing the solution by means of a peristaltic pump:

320   (6) laboratory metal determination by ICP-MS in both the sample and strip solutions.

321

322   2.5. Accuracy tests

323   To ascertain accuracy and to assure comparability of data produced during the cruise, analytical quality control of Cd,

324   Pb and Cu measurements were carried out by analysing several certified reference materials (the SLEW-3 for estuarine

325   water, the CASS-4 for nearshore seawater, and the NASS-5 for open seawater) with all the instrumentations available.

326   Certified reference materials were UV irradiated prior to analysis, as for the seawater samples collected.

327   The results of the systematic measurements carried out on reference materials during the entire period of work, using

328   all the instrumentations available on board and in laboratory, gave ($n = 5$-7) mean values (± SD) of SLEW-3, Cd

329   0.43 ± 0.01 nmol L^{-1}; Pb 0.046 ± 0.010 nmol L^{-1}; Cu 20 ± 2 nmol L^{-1}; CASS-4, Cd 0.24 ± 0.02 nmol L^{-1}; Pb 0.045 ± 0.008

330   nmol L^{-1}; Cu 9.3 ± 0.8 nmol L^{-1}; NASS-5 Cd, 0.21 ± 0.02 nmol L^{-1}; Pb 0.038 ± 0.006 nmol L^{-1}; Cu 4.6 ± 0.3 nmol L^{-1},

331   against certified mean values (± 95% confidence interval) of SLEW-3 Cd 0.43 ± 0.04 nmol L^{-1}; Pb 0.043 ± 0.007 nmol

332   L^{-1}; Cu 24 ± 2 nmol L^{-1}; CASS-4 Cd 0.23 ± 0.03 nmol L^{-1}; Pb 0.047 ± 0.017 nmol L^{-1}; Cu 9.3 ± 0.9 nmol L^{-1}; NASS-5

333   Cd 0.20 ± 0.03 nmol L^{-1}; Pb 0.040 ± 0.003 nmol L^{-1}; Cu 4.7 ± 0.7 nmol L^{-1}. Results were in good agreement with certified

334   reference values within the experimental errors, showing a good accuracy of all the measurements.

335

336   2.6. Inter-comparison exercises

337   During the cruise, laboratory and field-based inter-comparison exercises of all the analytical techniques available were

338   carried out, in order to validate the developed analytical tools with common analytical procedures. Three principal types

339   of field-based inter-comparisons were carried out: (i) the comparison between the different dynamic fractions determined

340   by the GIME sensors available on board; (ii) the comparison between the total and the total HCl-extractable concentrations

341   measured by conventional instrumentations, on one side, and the in-situ total acid extractable concentration measured by

342   the GIME-FIA system, on the other; and (iii) the comparison between the free metal ion concentrations determined by

343   the CGIME sensor and the HF-PLM technique. Some results of the inter-comparison exercises were reported in

344   Braungardt et al. (2009) and Tercier-Waeber et al. (2005). Braungardt et al. (2009) compared the metal dynamic

345   concentrations measured at 5-m depth of the first two stations of the study transect. Tercier-Waeber et al. (2005) compared

346   the results obtained by the in-situ application of the GIME-FIA and the total content measured by the conventional

347   Metrohm instrumentation. Here we extended the comparison between the different voltammetric instrumentations to all

348   the samples collected during the cruise. Results are fully reported in the Supporting Information (Text S2; Tables S1 and

349   S2).

350   As shown in Table S1, a general good agreement was observed between the dynamic fraction data measured by

351   different VIPs available on board. Cd dynamic fraction determined by the VIP-A represented the only exception, showing

352   at the surface very high values, probably related to laboratory contamination. Concerning the total concentrations (see

353   Table S2 in the Supporting Information), although some high values due to possible contamination problems, the in-situ

354   total extractable fraction measured by the GIME-FIA procedure was often consistent with the total metal concentration

355   for Pb. On the contrary, the in-situ total extractable fraction of Cu was comparable to the total acid-extractable fraction

356   measured by conventional Metrohm instrumentation. The few data of GIME-FIA available for Cd were higher than the

357   total concentrations, probably due to contamination problems.

358   The very few data obtained for the free metal ion concentration by the CGIME sensor (values available only for Cu)

359   seemed to be in agreement with values measured by the HF-PLM technique.

360

361   2.7. Ancillary measurements

362   At each station of the 2002-Adriatic cruise transect, continuous water column profiles (vertical resolution of 0.5 m),

363   were sampled for the master hydrographic variables (i.e. temperature, salinity, dissolved oxygen, oxygen saturation, pH,

364   redox potential) using a CTD probe fitted with a fluorometer for the chlorophyll-a vertical profile.

365   Temperature and salinity data obtained from the CTD measurements were used to calculate the density (ρ), and the

366   water column stability. The latter is proportional to the Brunt-Värsälä buoyancy frequency $N^2(z)$, which represents the

367   strength of density stratification (Agusti and Duarte, 1999). The depth at which the Brunt-Värsälä buoyancy frequency

368   was estimated to be maximal, which also corresponds approximately to the middle of the pycnocline, represents the Upper

369   Mixed Layer (UML). The value of $N^2(z)$ was also taken as a stability index of the water column (i.e. what it is commonly

370   called pycnocline strength).

371   At each station, several discrete samples were also collected at different depths for the determination of turbidity,

372   dissolved organic carbon (DOC), dissolved inorganic nutrients (nitrate$-NO_3^-$, nitrite$-NO_2^-$, ammonium$-NH_4^+$,

373   orthophosphate$-PO_4^{3-}$ and orthosilicate$-Si(OH)_4$), and phytoplankton abundance and composition. Nutrient

374   concentrations were measured following modified procedures developed by Strickland and Parsons (1972). Detailed

375   description of the nutrient analysis is reported elsewhere (Campanelli et al., 2012; Marini et al., 2008). Total dissolved

376   inorganic nitrogen (DIN) was calculated as the sum of the NO_3^-, NO_2^- and NH_4^+ concentrations.

377   The analysis of phytoplankton was carried out following the Utermöhl method (Edler and Elbrachter, 2010).

378   Immediately after collection seawater samples were preserved in dark glass bottles by adding 0.8% formaldehyde

379 neutralized with hexamethylenetetramine and stored at 4 °C. In laboratory, 40-100 mL sub-samples were homogenized,

380 settled in a cylinder-chamber complex and then observed using the inverted microscope. During counting procedure, 30

381 random fields were examined at 400-x magnification. All phytoplankton cells larger than 2 μm were identified and

382 counted. Then the entire chamber was observed at 200-x to assess the larger and less frequent organisms. Bio-volume

383 was measured to evaluate the biomass (expressed in μg C L^{-1}) following Menden-Deuer and Lessard (2000).

384

385 2.8. Statistical analysis

386   Countered sections are plotted using master variable and nutrient data that were gridded using the Data-interpolating

387 Variational Analysis (DiVA) coupled to the software Ocean Data View 4.7.10 (Schiltzer, 2017).

388   Experimental data were elaborated by principal component analysis (PCA), which was carried out on standardized

389 data; significant components were obtained through the Wold cross-validation procedure (Wold, 1978). The 5 m samples

390 of Stns. 1 and 2 were excluded from the dataset, because only the dynamic fractions were determined at this depth. Only

391 three depths of Stn. 6 (0.2 m, 5m and 25 m) were considered, since metal dynamic fractions were measured only at those

392 depth The high (contaminated) values of dynamic Cd were substituted by the HCl-extractable dissolved fraction (obtained

393 by filtering seawater samples on 0.45 μm pore membranes, acidifying with superpure HCl 2:1000 and analysing without

394 UV pre-treatment) which was very close to the Cd dynamic fraction (see data in Supplementary Information, Table S3),

395 and when this fraction was not available (we determined HCl-extractable dissolved fraction only in surface samples), the

396 dissolved Cd values (10- and 15-m depth values of Stn. 3) were used. The free metal ion concentrations were also

397 excluded, because of the very few and sporadic results obtained. The statistical analysis and the PCA were carried out

398 using Statistica package (StatSoft; vers. 8.0), and the differences were deemed statistically significant at $p<0.05$.

399

400

401

402 **3. Results**

403

404 3.1. Hydrography, dissolved nutrients and phytoplankton

405   Data on the master hydrographic variables, dissolved organic carbon (DOC), dissolved nutrients and phytoplankton

406 obtained during the cruise in the 2002-Adriatic Sea cruise are shown in Figures 2-4, S1 and Table S4.

407   Temperature and salinity varied from 16.28°C to 19.74°C and from 25.50 to 38.90, respectively (Fig. 2). Density

408 anomalies varied from 18.12 kg m^{-3} to 28.66 kg m^{-3} (Fig. S1). Temperature varied within a narrow range (up to 18%

409 variability), thus density variations were essentially due to salinity variations (also confirmed by the high positive

13

correlation coefficient, $r = 0.9798$, Tab. S4). Within the Po River plume, a stratification of the water column was observed with a very shallow UML (up to 5-m depth) and with a sharp salinity gradient. At this depth, the pycnocline showed a high strength ($N^2(z) = 557 \times 10^{-4}$ s^{-2}), which progressively decreased seawards. In the marine area (Stn. 6) water column became quite homogeneous, the UML extended deeper (~50 m), the halocline disappeared, while the thermocline still persisted and was responsible of a very weak pycnocline ($N^2(z) = 15 \times 10^{-4}$ s^{-2}) (Fig. 2).

Dissolved oxygen showed concentrations in the range $3.5 - 11$ mg L^{-1}, slightly over saturation levels (100%) with percentages ranging between 100 and 138% within the stratified layer (except for Stn.1, Fig. 2). Then, it gradually decreased down to the bottom reaching saturation values of ~60%. Values slightly lower than 50%, indicative of hypoxia, were observed only at the Stn. 5 close to the bottom, while in the marine area, dissolved oxygen showed a homogenous vertical distribution and well-oxygenated waters (~100% of saturation). Along the longitudinal profile, dissolved oxygen values (as well as saturation percentages) showed a surface maximum at Stn. 4, after which it decreased seawards to values very close to those of the pro-delta stations.

pH ranged from 7.94 to 8.39 and showed a longitudinal profile similar to that observed for dissolved oxygen (Fig. 2). In the pro-delta area, pH slightly decreased with depth, except in Stn.1 where it showed an opposite trend in the water column. In the frontal and marine areas, pH remained almost constant within the mixed layer, and then it sharply decreased with depth, even though at the Stn. 6 this decrease was less marked (Fig. S1).

Turbidity was high (~16 NTU) near the Po mouth, but sharply decreased seawards reaching values close to the detection limit of the instrument. In all the stations studied, turbidity showed a similar trend in the water column; it decreased with depth, but proceedings seawards, higher values (sometimes 2-3 times higher than the surface) were recorded, in the proximity of the bottom (Fig. S1).

Chlorophyll-a (Chl-a) concentration measured *in situ* by the CTD probe ranged between 0.3 and 13.3 mg L^{-1} and sharply decreased seawards. A clearly defined deep chlorophyll maximum (DCM) of ~10 mg m^{-3} was observed, closely following the pycnocline. In the marine area, Chl-a vertical distribution was homogeneous with very low values, ~0.3 mg L^{-1} (Fig. 3).

The total phytoplankton abundance ranged between 8.3×10^6 cell L^{-1} and 3.4×10^5 cell L^{-1} (Tab. S4). Spatial distribution of micro-phytoplankton showed a general seaward-decreasing trend, even if a peak (principally due to diatoms) of abundance was observed in the frontal area, with densities similar to those of the stations closer to the Po mouth. The most abundant groups were represented by diatoms and phytoflagellates (ranging from 0.014 to 4.8×10^6 cells L^{-1} and from 0.25 to 3.8×10^6 cells L^{-1}, respectively, Tab. S4) in agreement with several previous studies on phytoplankton composition in the northern Adriatic Sea (Totti et al., 2005).

14

440   DOC concentrations decreased along the Po plume, with values that ranged between ~ 140 μmol L^{-1} at the Po mouth

441   and ~ 60 μmol L^{-1} in open sea, with a variation of ~60% (Fig. 3). This horizontal decreasing trend of DOC was also

442   observed in the water column, with bottom values that were 40-60% lower than those of the surface. This distribution

443   changed in the marine area, where after a slightly increase within the first 15-m depth, it was quite homogeneous down

444   to the bottom.

445   DIN (ranging from ~1 μmol L^{-1} to ~90 μmol L^{-1}) and orthosilicates, $Si(OH)_4$ (ranging from 0.02 to 42 μmol L^{-1})

446   showed a decreasing trend (~98%) seawards (Fig. 4). DIN was represented for the most part by nitrates (60-100% of the

447   total). A very small fraction (ranging from 0.1% to ~15%) of the DIN was represented by ammonium, while nitrites

448   represented a more remarkable quote (1-40% of the total). Both DIN and orthosilicates were characterized by a general

449   drawdown of concentrations within the stratified layer. This decreasing trend was more marked in the stations closer to

450   the Po, because of the river influence. Afterward, concentrations remained almost constants with depth, while at the

451   bottom they arose again (the anomalous high seafloor value of nitrates at Stn. 6 was probably due to contamination

452   problems, and thus, it was not considered in the computation of DIN) (Fig. 4).

453   Orthophosphates were generally low, with values ranging from 0.04 μmol L^{-1} to ~0.12 μmol L^{-1}. They showed an

454   opposite trend with respect to nitrogen species and silicates, concentrations increasing of ~50% along the transect (Fig.

455   4). Phosphate distribution in the water column varied greatly from station to station. In Stns. 1 and 3 it increased gradually

456   with depth, while at Stn. 2 a gradual decrease was observed. From Stn. 4 to the open sea, phosphates showed a maximum

457   at the pycnocline; afterwards they slightly decreased down to the bottom.

458

459

460   3.3. Metal speciation

461   The distribution of the different metal fractions along the study transect is reported in Figures 5-8, divided for each metal

462   and for each sampling station. Total, dissolved, particulate, dynamic and colloidal concentrations are given for each

463   element. Also free-ion metal concentrations are discussed, even if these data are reported only in Tab. S2, due to the

464   paucity of the values measured. Data on dynamic fraction are the mean of measurements carried out by each of the VIP

465   systems available on board, with the exception of contaminated samples. It is to be noted that preliminary results on free

466   metal ion concentrations have been previously reported in Tercier-Waeber et al. (2005). Here, we provide a more

467   exhaustive description which includes such data presented previously, as well as the comparison with the other metal

468   fractions and master variables. The metal concentrations here measured are also compared to literature data obtained from

469   several estuaries, deltas, coastal and oceanic waters, worldwide (Table 1).

15

470

471   3.3.1. Cadmium

472   The Cd content in the waters of the transect was very low with an overall mean (interquartile range) of 0.14 (0.11 –

473   0.16) nmol L^{-1}. Our values are lower than those recorded in previous surveys in the same area and in other Italian rivers,

474   while they are similar to Cd concentrations measured in the whole basin of the Adriatic Sea and in general in the

475   Mediterranean Sea. Further, our values are as in the same order of magnitude as those found elsewhere in European

476   estuaries and, in general, as those measured in oceanic waters worldwide (Tab. 1).

477   A general longitudinal decreasing trend can be observed seaward for all the Cd fractions detected (Fig. 5a). Dissolved

478   Cd (from 0.068 nmol L^{-1} to 0.25 nmol L^{-1}) constituted the most important fraction of the total (concentrations ranging

479   between 0.080 nmol L^{-1} and 0.26 nmol L^{-1}). The only exception was present in the stations closer to the Po mouth, where

480   a more marked contribution by particulate fraction can be detected, though Cd$_{diss}$ percentages remained still high (70-90%)

481   of the total). The vertical profile of dissolved Cd showed an almost homogeneous behaviour over the transect, with a

482   maximum (excepting in the pro-delta area) at the DCM (5-10 m depth).

483   Apart from the high values at the surface of Stns. 2, 4 and 6 and at the bottom of Stn. 3, due to possible contamination

484   problems, the Cd dynamic fraction accounted for ~40% to ~100% of Cd$_{diss}$ (values ranging from 0.05 nmol L^{-1} to 0.20

485   nmol L^{-1}). The percentage of this fraction with respect to the dissolved concentration was high (90-100%) in the pro-delta

486   area, while it decreased seawards within the UML, reaching in the open sea values about half to the Cd$_{diss}$ (Fig. 6). Below

487   the pycnocline, the concentration of Cd$_{dyn}$ increased down to the seafloor, where its percentage was again 90-100% of

488   Cd$_{diss}$. In the open sea, a quite homogeneous distribution of Cd$_{dyn}$ with depth was observed, with a contribution to the

489   dissolved fraction of about 60-70%. An opposite trend was observed for the colloidal Cd fraction, that increased seaward,

490   reaching values ~40-50% of Cd$_{diss}$, and sharply decreased with depth to values close to zero (Fig. 6).

491   Free Cd-ion [Cd^{2+}] concentrations were found to be below the detection limit (~60 pmol L^{-1}, as reported in Noël et

492   al., 2006) for both the CGIME sensor and the HF-PLM system (Tab. S-2).

493

494   3.3.2. Lead

495   Lead speciation changed greatly along the transect (Fig. 5b and Fig. 7). The total concentration of Pb was generally

496   high at the Po river mouth (~1.4 nmol L^{-1}) and then decreased seaward, to reach asymptotically an open sea value of

497   ~0.2 nmol L^{-1}, with an 85% decreasing trend. At the surface of the pro-delta and frontal areas, Pb content was dominated

498   by the particulate fraction (accounting for ~70% of the total), since dissolved Pb showed low concentrations (~0.40 nmol

499   L^{-1}). Pb$_{diss}$ initially decreased in the frontal area, passing from ~0.4 nmol L^{-1} at the Po River mouth to ~0.09 nmol L^{-1} up

16

500   to ~30 km off shore from the river. Proceeding seaward, it increased both in absolute and in relative terms reaching values

501   close to those of the Pb_{tot} (~0.2 nmol L^{-1}). Therefore, Pb_{part} greatly decreased along the Po plume, reaching values close

502   to zero in the marine area. Both the total and the dissolved Pb concentrations were in good agreement with data reported

503   in the literature for the same area and for other rivers worldwide (Tab. 1). Obviously, our data are higher than those

504   referred to oceanic waters (sometimes about one order of magnitude) with the exception of the seawater end-member

505   values, which fall within the same order of magnitude of literature data.

506   In the water column, Pb was mainly present in its dissolved form (70 – 100% of the total) which was also responsible

507   of the maximum of Pb_{tot} at the DCM (5-10 m depths). The particulate fraction returned significant at the seafloor, where

508   its contribution to the total increased up to ~70%.

509   The dynamic fraction of Pb ranged between ~0.02 nmol L^{-1} and ~0.2 nmol L^{-1}. In general, Pb_{dyn} represented a very

510   small and constant fraction of the Pb_{diss} (~15-20%) within the first 10 km far from the Po mouth, further offshore it greatly

511   increased in both its concentration and percentage reaching at the surface values up to the 50% of the dissolved

512   concentration. The contribution of Pb_{dyn} with respect to the dissolved concentrations increased with depth in the stations

513   close to the Po mouth, while it decreased in the water column with the increasing of the distance from the river. Hence,

514   the colloidal fraction of Pb was dominant (~80% of the Pb_{diss}) in the pro-delta area and then decreased in the open sea to

515   values half of those of Pb_{diss} (Fig. 7).

516   The free-ion Pb fraction (no CGIME data are available) showed very low concentration, varying from about 2 pmol L^{-1}

517   near the Po river to ~10 pmol L^{-1} in the open sea (Tab. S-2). It represented a few percentages of the Pb_{diss} (from ~1% to

518   ~10%), but the contribution to Pb_{dyn} was much higher (from ~5% to ~40%). Due to the very few data available for this

519   fraction, we are not able to describe in details the behaviour of [Pb^{2+}] in the study area. We can only observe an increasing

520   trend of [Pb^{2+}], both in absolute and in relative terms with the distance from the river and with depth.

521

522

523   3.3.3. Copper

524   Copper showed a marked decreasing trend of all the fractions along the study transect (Fig. 5c, 8).

525   Total Cu concentration varied from ~3 nmol L^{-1} to ~20 nmol L^{-1}, and it mainly constituted of the dissolved fraction

526   that ranged from 2 nmol L^{-1} to ~11 nmol L^{-1}. The contribution of Cu_{diss} to Cu_{tot} at the surface increased along the study

527   transect, Cu_{diss} being ~100% of the total in the open sea. Both total and dissolved Cu values are similar to those recorded

528   in previous surveys for the northern and central Adriatic Sea (Tab. 1), with the only exception of Tankere et al., 2000 who

529   reported Cu higher values. For the Southern Adriatic Sea and the rest of the Mediterranean Sea (Tankere and Statham,

17

530 1996) lower values have been reported as well as for the oceanic waters (Tab. 1). Dissolved Cu concentrations were

531 generally lower than those measured in other European estuaries and than the average value of the rivers worldwide (Tab.

532 1).

533   A vertical decreasing trend of Cu_{tot} was also observed within the Po plume. At the boundary of the frontal area (Stn.

534 5) and in the marine area, Cu_{tot} showed a maximum in the upper 10-15 m of the water column, and then it remained almost

535 constant with depth (Fig. 8). Moreover, Cu_{diss} decreased within the stratified layer; and below it remained almost constant

536 down to the seafloor with values close to Cu_{tot}. Therefore, the Cu_{diss} proportion increased with depth reaching values up

537 to ~90% of the total. Total particulate Cu was high at the surface in the stations of the pro-delta and decreased seaward

538 and with depth reaching low values (up to ~30% in the open sea) (Fig. 8).

539   As for Pb, the dynamic fraction of Cu represented a small fraction (up to ~50% Fig. 5c) of the dissolved concentration,

540 with values ranging between ~0.15 and ~4.0 nmol L^{-1}. The fraction of dissolved Cu associated to colloidal material was

541 much more significant (~70-100% of the Cu_{diss}). Both Cu_{dyn} and Cu_{coll} concentrations decreased seaward, but the

542 contribution of the Cu_{coll} to the dissolved Cu slightly increased along the transect (Fig. 5c).

543   Considering the water column, Cu_{dyn} decreased at all the stations within the stratified layer (with the exception of Stn.

544 5 where a maximum at 5-m depth was observed); afterwards it remained almost constant down to the seafloor (Fig. 8).

545 The proportion of Cu_{dyn} *vs.* Cu_{diss} was ~30% within the stratified layer, for all the stations, and then it drastically fell to

546 ~7% near the seafloor. Also Cu_{coll} decreased within the stratified layer, but contrary to Cu_{dyn}, below the pycnocline it

547 increased with depth. Its percentage to Cu_{diss} was generally higher than Cu_{dyn} and slightly increased in the water column.

548 In the marine area (Stn. 6), although the very few data available on dynamic Cu, a sub-surface decrease and a subsequent

549 homogeneous distribution with depth can be recognized (Fig. 8).

550   The Cu free-ion fraction measured by the CGIME sensor showed very low values ranging between ~0.03 nmol L^{-1} to

551 ~0.62 nmol L^{-1} (Tab. S-2). [Cu^{2+}] decreased by ~95% along the transect, as well as the proportion of this fraction with

552 respect to the dissolved concentration decreased by ~90% seawards. Data available for this fraction are scarce, thus a

553 proper description of Cu_{free} variation in the water column cannot be defined, even if an apparent decrease can be noted.

554

555

556 3.4. Multivariate statistical data analysis

557   The correlation matrix (Pearson's linear coefficients) is reported in Table S5.

558   Among nutrients, only NO_3^- and $Si(OH)_4$ co-varied positively (highly significant correlation), whereas PO_4^{3-} showed

559 no correlations with the other nutrients, even in the surface layers. Chl-a was associated with O_2, pH, total phytoplankton

18

abundance and biomass and negatively correlated with phosphates. Total phytoplankton abundance and biomass were in contrast with the main hydrographic parameters (depth, temperature, salinity and density) and with the distance from the Po, while they were positively correlated with turbidity and DOC.

Nearly, all the metal fractions were in contrast with salinity (although some of the correlations were not significant), indicating the influence of the river waters on their distribution, as subsequently confirmed by PCA (see below). Only Pb_{dyn} and Cd_{coll} showed a different behaviour, co-varying (but not significantly) with salinity. Both Cd and Cu (excepting Cd_{part} and Cd_{coll}) showed significant correlations with phytoplankton abundance and biomass. Pb_{tot} was positively correlated with phytoplankton community, as well. Moreover, Cd_{diss} was correlated positively only with nitrogen species, while Cd_{dyn} co-varied with silicates and not with nitrates. Pb_{dyn} showed no significant correlations with any physical, chemical or biological variable, while Pb_{tot} was statistically correlated with NO_2^- and $Si(OH)_4$, and Pb_{diss} with NH_4^+. Cu was strong correlated with $Si(OH)_4$ and, partly (only Cu_{tot} and Cu_{part}) with NO_3^-. No significant correlations were found between any of the metals and PO_4^{3-}, overall. All Cu fractions were correlated with total, dissolved and dynamic Cd (excepting Cu_{part} which was not correlated with Cd_{tot} and Cd_{diss}), and with the total and particulate fractions of Pb, indicating that they are affected by the same factor.

To better understand the effect of the Po River on the metal species distribution, a multivariate analysis (PCA) was performed to reduce the dimensionality of the dataset to few components that summarize the information contained iin the overall dataset.

The PCA applied to the standardized variables, led to the identification of three significant, cross-validated principal components (PCs) counting for about 68% of the total variation. Figure 9 shows the results of the PCA in terms of loading plot (Fig. 9a) and score plot (Fig. 9c) of PC1 vs. PC2 and in terms of loading plot (Fig. 9b) and score plot (Fig. 9d) of PC2 vs. PC3.

The first principal component (explained variance 42%, Fig. 9a, 9c) is strongly associated to the main hydrographic parameters (temperature, salinity, density) and to the distance from the Po mouth (positive loadings), which are in contrast with NO_3^-, $Si(OH)_4$, turbidity, DOC and the main phytoplanktonic groups (diatoms and phytoflagellates). This group of variables (nutrients and phytoplankton community) includes also all the metals and almost all the metal fractions (even if not all have high loads on PC1), with the exception of Pb_{dyn} and Cd_{coll}, that showed positive loadings on PC1. Thus, the PC1 expresses the effect of the river outflow on the distribution of metal species, nutrients and main phytoplankton communities. Quite surprisingly, phosphates were associated to salinity gradient and in contrast with the general trend of other nutrients and metals. PC2 (explained variance 16%, Fig. 9a) is associated to O_2, pH, dinoflagellates, Cd_{coll}, coccolithophorids, Chl-a and NH_4^+ (positive loadings). All these variables are in contrast with NO_2^- and, to a lesser extent

with silicates, Pb_{part} and turbidity. Hence, the second principal component expresses the biological activity and regeneration processes (see the score plots, Fig. 9c). The third component (explained variance 10%, Fig. 9b, 9d) is dominated by the speciation of dissolved Pb with the contrast between Pb_{diss}, and Pb_{coll}, on one side, and Pb_{dyn} (together with DOC) to the other side. The third principal component expresses the role of the organic matter on the dissolved Pb speciation.

4. Discussion

4.1. Environment

The oceanographic cruise along the Po plume (October-November 2002) was carried out after a particularly rainy period. The mean daily discharge measured at the hydrometric station of Pontelagoscuro (located at 80-km before the Po River mouth) was around 1300 m^3 s^{-1} (ARPA Emilia-Romagna, 2002), similar to the long-term average for the period of 1828 m^3 s^{-1} (Boldrin et al., 2005; Campanelli et al., 2012). However, the cruise was preceded by a particularly rainy period, where the Po river discharge reached values up to 3000 m^3 s^{-1} (ARPA Emilia-Romagna, 2002). Consequently, the influence of the Po River, in terms of reduced salinity at the surface, was evident about 50-km offshore from the mouth. This resulted in a marked horizontal stratification of the water column, highlighted by the presence of thermocline, strong halocline and pycnocline ($N_2(z)$ ~400 × 10^{-4} s^{-2}) throughout most part of the transect. In the open sea, the effect of the Po outflow disappeared, as well as the stratification of the water column sharply reduced ($N_2(z)$ up to 15 × 10^{-4} s^{-2}, at 50-m depth of Stn. 6).

Principal component analysis applied to the whole dataset revealed that surface waters of the frontal area were affected by other factors than the Po river runoff (Fig. 9). These stations were associated with oxygen super-saturation levels (up to ~140%), high value of pH and NH_4^+, corresponding to phytoplankton abundance and biomass peaks. Although diatoms were mainly responsible of total phytoplankton abundance and biomass distribution (see below), a dramatic increase (~80%) of both dinoflagellates and coccolithophorids occurred in the frontal area, while in the other stations these groups were practically absents (especially coccolithophorids). We hypothesize that saltier, well-oxygenated and high productive waters originated by the northern part of the Adriatic Sea (and maybe moved by winds) intrude in the frontal area and proceeded southward. Unfortunately, wind data of that period are not available, hence we are not able to corroborate this hypothesis.

20

620   DOC concentrations were similar to those typical of the region during the autumn. They were positively correlated

621   with both phytoplankton abundance and biomass, highlighting that phytoplankton significantly contributed to DOC rather

622   than the Po River. In the water column, DOC sharply decreased within the stratified layer, then below the pycnocline it

623   showed a quite uniform profile, reaching values very close to the background levels (76 ± 10 µmol L^{-1}) found by Pettine

624   et al. (2001) in this area and typical of the surface oceanic waters (Guo et al., 1995).

625   Nutrient distributions along the transect highlighted the role of the Po River discharge and that of the biological

626   processes in controlling the nutrient levels in the Northern Adriatic Sea as already observed in previous surveys (Boldrin

627   et al., 2005; Grilli et al., 2005; Campanelli et al., 2012). Nutrient concentrations are typical of the autumn season for the

628   Northern Adriatic Sea (Boldrin et al., 2005; Campanelli et al., 2012) and showed a clearly seaward decreasing gradient.

629   The nutrient vertical profiles were generally characterized by high surface concentrations (especially in the pro-delta and

630   frontal areas), decreasing down to a depth of about 5-10 m (within the stratified layer), a trend opposite to that of the

631   salinity, highlighting the influence of the Po river input. Below the 10-m depth concentrations were vertically uniform or

632   increased with depth.

633

634

635

636   4.2. Metal speciation along the Po River plume

637   Several processes, both internal (i.e. trace metal removal from the dissolved phase by adsorption, precipitation and

638   co-precipitation of solutes, or by flocculation and net sedimentation with suspended matter, or by biological uptake;

639   production of trace metals in the dissolved phase by desorption or solubilisation of particulate matter; transformation and

640   migration of trace metals at the sediment/water interface) and external (mainly anthropogenic activities, such as, pollution,

641   discharging of pollutants or cooling waters) control the speciation and the distribution patterns of metals in the mixing

642   zone between salt and fresh waters. These processes are affected, in turn, by the strong longitudinal variations in physical,

643   chemical and biological parameters that develop in estuarine systems.

644   Principal component analysis reveals a strong influence of the Po River outflow on the spatial and vertical distribution

645   of Cd, Pb and Cu species. Almost all the metal fractions linearly decreased with salinity gradient, consequently to dilution

646   effect (i.e. all the metal showed conservative behaviours). Although all the metal fraction contents globally decreased

647   with salinity, speciation distribution patterns significantly differed from one metal to another.

648   Cd was mainly present in its dissolved form (particulate fraction up to 20% of the total). The contribution of Cd

649   particulate fraction increased within the stratified layer, following the maximum phytoplankton abundance. Below the

21

650 pycnocline, dissolved/particulate fractionation changed again, due to remineralisation processes from dead phytoplankton

651 cells, that released Cd in seawater (Bruland and Lohan, 2003).

652 Concerning Pb and Cu, the particulate fractions of the two metals were dominant within the pro-delta area (accounting

653 for ~70% of the Pb_{tot} and for ~55% of the Cu_{tot}), while the dissolved fractions were mainly presents in the open sea.

654 Nevertheless (with the exception of the pro-delta area), Cu partitioning was dominated by the dissolved fraction

655 throughout the study transect. Contrary to its oceanic "hybrid" distribution in the water column (e. g. surface depletion,

656 linear increase with depth and deep scavenging by particles) (Bruland and Lohan, 2003; Jacquot and Moffet, 2015),

657 dissolved Cu remained elevate all the way down to the bottom. Only at the seafloor of the frontal area, an increase of Cu

658 content occurred, suggesting additional inputs from sediments (such as re-suspended sediments), as observed in open

659 ocean waters (Tankere et al., 2000; Waeles et al., 2008; Jacquot and Moffett, 2015).

660 Depth profile of Pb confirmed its nature of particle-reactive metal. Because of desorption processes from the

661 particulate matter, dissolved Pb concentrations increased along the water column, while the particulate fraction became

662 again significant in proximity of the seafloor. In fact, sediment can be considered as an additional source of particulate

663 Pb due to several biogeochemical processes within the sediments themselves and at the sediment/water interface (Tankere

664 et al., 2000; Cobelo-Garcia and Prego, 2004).

665 Differences between Cd, on one hand, and Pb-Cu on the other hand, were observed also for the dissolved-fraction

666 speciation. Cd was mainly present as dynamic fraction in the pro-delta area. In the remaining part of the transect, the

667 contribution of the colloidal fraction to the dissolved Cd became more and more important within the stratified layer, up

668 to 40-50% of Cd_{diss} in the marine area. As observed by Baeyens et al. (1998) in the Scheldt estuary (Netherlands), it seems

669 likely that the production of dissolved Cd contributed to the dynamic fraction (potentially bio-available) near the Po

670 mouth, afterwards it decreased in favour of less dynamic species, i.e. colloidal species. Martin et al. (1995) in the Venice

671 Lagoon, also found similar colloidal contribution (30-40%) to the dissolved Cd, as well as in the Ochlockonne estuary

672 (Powell et al., 1996) or in the Scheldt estuary (Baeyens et al., 1998). As reported by Comans and Van Dijk (1988), the

673 speciation of Cd is generally dominated in estuaries by stable and soluble chlorocomplexes, but in some systems, organic

674 complexation could be important, as well. As showed in the PCA (Fig. 9), Cd_{coll} is significantly associated with small

675 algal cells, the dinoflagellates and the coccolithophorids, which increased in the frontal area of a percentage much higher

676 (80-98%, respectively) than diatoms (~40%) or phytoflagellates (see in Section 4.1). Thus, the increase of colloidal Cd

677 seawards could be ascribed to the complexation with algal cells or with exudates produced by phytoplankton, as well.

678 Below the pycnocline and down to the bottom, Cd_{diss} returned to be mainly constituted by the dynamic fraction (90-100%

679 of the Cd_{diss}), following the release of this fraction from phytoplankton dead cells that sedimented in the water column.

22

680   Dissolved Pb and Cu speciation was dominated by colloidal fraction (40 – 95% of the dissolved fraction for both

681   metals). The low proportion of Pb_{dyn} and the consequently strong association of Pb with colloidal material was in

682   agreement with previous studies (Martin et al., 1995; Waeles et al., 2008; Braungardt et al., 2011). For example, Martin

683   et al. (1995) reported that colloidal Pb accounted for up to ~90% of the total dissolved Pb in the Venice Lagoon (northern

684   Adriatic Sea). Scarponi et al. (1995) during speciation studies carried out through voltammetric titration procedures in

685   seawater of different areas (e.g. Adriatic Sea, Antarctic Ocean, and North Eastern Pacific) found that the ASV-labile

686   fraction (similar to our dynamic fraction) accounted for about 15% of the total Pb at the surface.

687   When considering the contribution of colloidal copper in various estuarine or delta systems disparate results were

688   obtained. As example, in the Danube and in the Loire estuaries (Waeles et al., 2004, 2009), Cu_{coll} accounted for only 10-

689   40% of the total dissolved metal. In the Penzé estuary (Waeles et al., 2008) or in the Restronguet Creek (Braungardt et

690   al., 2011) the colloidal fraction showed percentages similar to our results. The high presence of colloidal Cu confirmed

691   results obtained in previous speciation studies carried out by Zago et al. (2002) in the Northern Adriatic Sea. The authors

692   did not detect labile metal concentrations of the two studied metals (Cu and Zn), but, computing the ligand concentrations,

693   they concluded that the total dissolved metal concentration of Cu was exclusively present as organically complexed

694   metals. Several speciation studies worldwide (Capodaglio et al., 1994; L'Her Roux et al., 1998; Waeles et al., 2004, 2008,

695   2009; Buck et al., 2007) suggested a model with two classes of ligand for both dissolved Pb and Cu, the strongest

696   consisting of detrital matter (e.g. fulvic and humic acids) and living biogenic material (living organisms, such as algae,

697   bacteria, virus, or organic exudates).

698   Since the phytoplankton highly contributed to the DOC pool (see section 4.1), it is plausible to hypothesise an organic

699   origin for Pb and Cu ligands in the northern Adriatic Sea. Further studies, including a better spatial resolution and

700   dissolved organic matter speciation are, therefore, necessaries to gain more insight into the speciation of the two dissolved

701   metals and the nature of Pb-Cu ligands in the Adriatic Sea.

702   The impact of the different processes controlling trace metal specie distributions along the Po plume can be established

703   also by investigating metal–nutrient relationships. In open ocean water, bioactive trace metals (Cd, Cu, Fe, Ni, Zn) have

704   positive relationships with limiting nutrients (PO_4^{3-} and $Si(OH)_4$), following the assumption that the metal:P slopes in

705   seawater should be equal to the ratios in which these elements are present in the cells; the so-called "extended Redfield

706   ratio" (Morel and Hudson, 1985). Deviations from this linear metal–nutrient relationship may be indicative of additional

707   inputs not observed in open ocean environments (Martin et al., 1980). In the present work, all the metal fractions did not

708   show significant positive correlations with PO_4 (Tab. S5). Similar ratios were observed also if surface values (which are

709   more affected by river discharge) were excluded (data not shown). The opposite gradients observed in the PCA between

710   metals and P (Fig. 9) cause the negative Me:P slopes recorded in these waters (Tab. S5), highlighting the influence of

23

711 other factors than biological cycles on metal distribution, i.e. the effect of the Po River discharge that masked, for

712 examples, the typical nutrient-like profile of Cd and Cu.

713

714

715 4.3. Significance of metal speciation

716   The dynamic metal concentrations here measured could offer some interesting insights on the toxic or limiting effects

717 of specific trace metals, since its peculiar characteristic to approximate the bio-available fraction (Buffle and Tercier-

718 Waeber, 2005) more than the dissolved fraction. Several studies have been carried out on assessing the toxicity of trace

719 metals on marine organisms, most of them dealing with the toxicity of the free metal ions. Very few is known about the

720 toxicity effect of the dynamic fraction. Studies based on laboratory cultures (Verweij et al., 1992; Perez et al., 2010)

721 reported that adverse effects on cyanobacteria and many marine phytoplankton species occurred for concentrations in the

722 range $0.001 – 0.1$ nmol L^{-1} for Cu^{2+}, $1 – 5$ nmol L^{-1} for Cd^{2+} and <0.1 nmol L^{-1} for Pb^{2+}.

723   Our dynamic Cd and Pb concentrations did not represent a risk to marine organisms in the Northern Adriatic Sea,

724 even if Pb showed concentrations very close or slightly below the thresholds previously reported. However, the Pb^{2+}

725 concentrations measured by the PLM technique (no data available from CGIME sensor) were few tens of pico-molar per

726 L (from 1 to ~15 pmol L^{-1}), far below the toxic levels measured in laboratory cultures. On the contrary, the dynamic

727 fraction of Cu showed values of the pro-delta (~4.0 nmol L^{-1}) being potentially toxic to 21 marine phytoplankton species

728 examined in laboratory cultures. Moreover, studies (Verweij et al., 1992; Beiras and Albentosa, 2004; Rivera-Duarte et

729 al., 2005) on the embryogenesis success of bivalves (*Mytilus galloprovincialis*, *Ruditapes decussatus*), sand dollar

730 (*Dendraster excentricus*), and sea urchin (*Strongylocentrotus purpuratus*) showed sensitivity towards Cu^{2+} at values of

731 EC_{50} (effective concentration of metal causing a 50% inhibition of embryos development with respect to the control)

732 ranged from ~0.06 nmol L^{-1} to ~0.16 nmol L^{-1}. Therefore, Cu dynamic fraction along Po plume showed concentrations

733 likely to be toxic to sensitive phytoplankton community and to have negative effects on larva development of coastal

734 macroinvertebrate species. Also Cu^{2+} concentrations (~0.3 nmol L^{-1}) at the Po mouth were higher than the EC_{50} values

735 provided for coastal macroinvertebrate larvae sensitivity to copper (Beiras and Albentosa, 2004), and that showed the

736 same order of magnitude of the toxic threshold range reported for plankton (Brand et al., 1986). In the case of copper,

737 hydroxy complexes are also believed to be toxic, with toxicity decreasing in the order, Cu^+ and $Cu^{2+} >$ inorganic

738 copper > organic copper (Allen and Hansen, 1996).

739   Moreover, culture studies have demonstrated that several metals may act synergistically or antagonistically to

740 influence growth limitation or toxicity to marine organisms (Annett et al., 2008; Semeniuk et al., 2009). In force of these

741 metal:metal antagonisms, elevated levels of free ions of one metal (e.g., Mn^{2+}) may alleviate the toxic effects of Cu^{2+}

742 (Sunda and Huntsman, 1983) or Zn^{2+} (Twining et al., 2011). Therefore, further studies including other metals in addition

743 to those of the present work are necessaries in order to gain more insight into metal speciation and potentially harmful

744 effects of metal species to marine organisms in the Northern Adriatic Sea.

745

746

747 **5. Conclusions**

748   The speciation of Cd, Pb and Cu was studied for the first time along the Po River plume. The oceanographic cruise

749 (Autumn 2002) was carried out after a particularly rainy period. Consequently, the influence of the river, in terms of

750 reduced salinity at the surface, was evident about 50-km offshore from the mouth. The distribution and speciation of Cd,

751 Pb and Cu in the Po River plume is mainly controlled by the river outflow.

752   Almost all the metal fractions linearly decreased with salinity gradient, consequently to dilution effect (i.e. all the

753 metal showed conservative behaviours). Cadmium was mainly present as dynamic fraction in the pro-delta area, while in

754 the remaining part of the transect, the contribution of the colloidal fraction to the dissolved Cd became more and more

755 important. On the contrary, the Pb and Cu partitioning was dominated by particulate fraction in the stations closer to the

756 Po mouth and by the dissolved fraction in the open sea. The colloidal fraction of these two metals constituted a significant

757 proportion of the dissolved concentration and it seems to be related to a biogenic origin. On the basis of speciation studies

758 on the dissolved organic matter in the Northern Adriatic Sea, we hypothesize a biogenic origin (small algae, or

759 phytoplankton exudates) of these colloidal fractions.

760   Metal concentrations measured in the present work are far below (at least one order of magnitude lower) the EQS

761 established by the Italian law (Italian DPR 172/15, 2015) in the enactment of the revised Priority Substances Daughter

762 Directive of the European Union, 2013/39/EU (2013), even if these Directives do not take copper into account at all (the

763 only national legal limit existing for Cu dates back to the Italian DPR 152/06 (2006), that established a threshold

764 concentration of 16 μmol L^{-1} referring to waters suitable to the life of salmonid and cyprinid organisms). However, our

765 Cu dynamic fraction along the Po plume showed concentrations likely to be toxic to sensitive phytoplankton community

766 and to have negative effects on larva development of coastal macroinvertebrate species. Also Cu^{2+} concentrations at the

767 Po mouth were higher than the EC_{50} values provided for coastal macroinvertebrate larvae sensitivity to copper.

768   The present work allows a better comprehension of the processes regulating marine biogeochemical cycles of trace

769 metals, it improve our insights on transport and fate of contaminants in the marine environment, giving valuable tools for

770 more reliable predictions of future changes and following actions to protect it, as recommended by the Marine Strategy

771 Framework Directive (descriptor 8th), (European Directive 2008/56/EC, 2008).

772

778   **References**

779   Agusti, S., Duarte, C.M., 1999. Phytoplankton chlorophyll a distribution and water column stability in the central Atlantic
780   Ocean. Oceanol. Acta, 22, 193–203.
781   Ahner, B.A., Morel, F.M.M., 1995. Phytochelatin production in marine algae. 2. Induction by various metals. Limnol.
782   Oceanogr., 40, 658–65.
783   Allen, H.E., Hansen, D.J., 1996. The importance of trace metal speciation to water quality criteria. Water Environ. Res.,
784   68, 42–54.
785   Annett, A.L., Lapi, S., Ruth, T.J., Maldonado, M.T., 2008. The effects of Cu and Fe availability on the growth and Cu:C
786   ratios of marine diatoms. Limnol. Oceanogr., 53, 2451–2461.
787   Annibaldi, A., Truzzi, C., Illuminati, S., Bassotti, E., Scarponi, G., 2007. Determination of water-soluble and insoluble
788   (dilute-HCl-extractable) fractions of Cd, Pb and Cu in Antarctic aerosol by square wave anodic stripping voltammetry:
789   distribution and summer seasonal evolution at Terra Nova Bay (Victoria Land). Anal. Bioanal. Chem., 387, 977–998.
790   Annibaldi, A., Truzzi, C., Illuminati, S., Scarponi, G., 2009. Recent sudden decrease of lead in Adriatic coastal seawater
791   during the years 2000-2004 in parallel with the phasing out of leaded gasoline in Italy. Mar. Chem., 113, 238–249.
792   Annibaldi, A., Illuminati, S., Truzzi, C., Scarponi, G., 2011. SWASV speciation of Cd, Pb and Cu for the determination
793   of seawater contamination in the area of the Nicole shipwreck (Ancona coast, Central Adriatic Sea). Mar. Pollut. Bull.,
794   62, 2813–2821.
795   Annibaldi, A., Illuminati, S., Truzzi, C., Libani, G., Scarponi, G., 2015. Pb, Cu and Cd distribution in five estuary systems
796   of Marche, central Italy. Mar. Pollut. Bull., 96, 441–449.
797   Aparicio-González, A., Duarte, C.M., Tovar-Sánchez, A., 2012. Trace metals in deep ocean waters: A review. J. Mar.
798   Syst., 100, 26–33.
799   ARPA Emilia-Romagna, 2002. Annali idrologici, Pt II.
800   Baeyens, W., Goeyens, L., Monteny, F., Elskens, M., 1998. Effect of organic complexation on the behavior of dissolved
801   Cd, Cu and Zn in the Scheldt estuary. Hydrobiologia 366, 81–90.
802   Baeyens, W., Leermakers, M., Gieter, M.D., Nguyen, H.L., Parmentier, K., Panutrakul, S., Elskens, M., 2005. Overview
803   of trace metal contamination in the Scheldt estuary and effect of regulatory measures. Hydrobiologia, 540, 141–154.
804   Beiras, R., Albentosa, M., 2004. Inhibition of embryo development of the commercial bivalves Ruditapes decussatus and
805   Mytilus galloprovincialis by trace metals; implications for the implementation of seawater quality criteria.
806   Aquaculture, 230, 205–213.
807   Belmont-Hebert, C., Tercier, M.L., Buffle, J., Fiaccabrino, G.C., de Rooij, N.F., Koudelka-Hep, M., 1998. Gel-Integrated
808   Microelectrode Arrays for Direct Voltammetric Measurements of Heavy Metals in Natural Waters and Other Complex
809   Media. Anal. Chem., 70, 2949–2956.
810   Bernardi Aubry, F.B., Gianpiero Cossarini, Acri, F., Bastianini, M., Bianchi, F., Camatti, E., De Lazzari, A., Pugnetti,
811   A., Solidoro, C., Socal, G., 2012. Plankton communities in the northern Adriatic Sea: Patterns and changes over the
812   last 30 years. Estuar. Coast. Shelf. Sci., 115, 125–137.
813   Boldrin, A., Langone, L., Miserocchi, S., Turchetto, M., Acri, F., 2005. Po River plume on the Adriatic continental shelf:
814   Dispersion and sedimentation of dissolved and suspended matter during different river discharge rates. Mar. Geol.,
815   222–223, 135–158.
816   Brand, L.E., Sunda, W.G., Guillard, R.R.L., 1986. Reduction of marine phytoplankton reproduction rates by copper and
817   cadmium. J. Exp. Mar. Biol. Ecol., 96, 225–250.
818   Braungardt, C.B., Achterberg, E.P., Axelsson, B., Buffle, J., Graziottin, F., Howell, K.A., Illuminati, S., Scarponi, G.,
819   Tappin, A.D., Tercier-Waeber, M.L., Turner, D., 2009. Analysis of dissolved metal fractions in coastal waters: An
820   inter-comparison of five voltammetric in situ profiling (VIP) systems. Mar. Chem., 114, 47–55.
821   Braungardt, C.B., Howell, K.A., Tappin, A.D., Achterberg, E.P., 2011. Temporal variability in dynamic and colloidal
822   metal fractions determined by high resolution in situ measurements in a UK estuary. Chemosphere, 84, 423–431.
823   Buck, K.N., Ross, J.R.M., Flegal, A.R., Bruland, K.W., 2007. A review of total dissolved copper and its chemical
824   speciation in San Francisco Bay, California. Environ. Res., 105, 5–19.
825   Buffle, J., Perret, D., Newman, M., 1992. The use of filtration and ultrafiltration for size fractionation of aquatic particles,
826   colloids, and macromolecules. In: Environmental Particles. Buffle, J.; van Leeuwen, H.P. (Eds.), Boca Raton, pp.
827   171–230.
828   Buffle, J., Tercier-Waeber, M.-L., 2005. Voltammetric environmental trace-metal analysis and speciation: from
829   laboratory to in situ measurements. Trace-Met. Anal., 24, 172–191.

830 Cabrini, M., Fornasaro, D., Cossarini, G., Lipizer, M., Virgilio, D., 2012. Phytoplankton temporal changes in a coastal
831   northern Adriatic site during the last 25 years. Estuar. Coast. Shelf Sci., 115, 113–124.
832 Campanelli, A., Grilli, F., Paschini, E., Marini, M., 2012. The influence of an exceptional Po River flood on the physical
833   and chemical oceanographic properties of the Adriatic Sea. Dyn. Atmos. Oceans, 52, 284–297.
834 Capodaglio, G., Toscano, G., Scarponi, G., Cescon, P., 1994. Copper complexation in surface seawater of Terra Nova
835   Bay (Antarctica). Int. J. Environ. Anal. Chem., 55, 129–148.
836 Cindrić, A.-M., Garnier, C., Oursel, B., Pižeta, I., Omanović, D., 2015. Evidencing the natural and anthropogenic
837   processes controlling trace metals dynamic in a highly stratified estuary: The Krka River estuary (Adriatic, Croatia).
838   Mar. Pollut. Bull., 94, 199–216.
839 Cobelo-Garcia, A., Prego, R., 2004. Chemical speciation of dissolved copper, lead and zinc in a ria coastal system: the
840   role of resuspended sediments. Anal. Chim. Acta, 524, 109–114.
841 Comans, R.N.J., Van Dijk, C.P.J., 1988. Role of complexation processes in cadmium mobilization during estuarine
842   mixing. Nature, 336, 151–154.
843 Donat, J.R., Lao, K.A., Bruland, K.W., 1994. Speciation of dissolved Copper and Nickel in South San Fransisco Bay: a
844   Multi-Method Approach. Anal. Chim. Acta, 284, 547–571.
845 Dorten, W.S., Elbaz-Poulichet, F., Mart, L.R., Martin, J.-M., 1991. Reassessment of the river input of trace metals into
846   the Mediterranean Sea. Ambio, 20, 2–6.
847 Edler, L., Elbrachter, M., 2010. The Utermöhl method for quantitative phytoplankton analysi. In: Karlson, B., Cusak, C.,
848   Bresnan, E. (Eds.), Microscopic and molecular methods for quantitative phytoplankton analysis. Intergovernmental
849   Oceanographic Commission of UNESCO, Paris, pp. 13–20.
850 European Parliament and Council, 2008. Directive 2008/56/EC of the 17 June 2008 establishing a framework for
851   community action in the field of marine environmental policy (Marine Strategy Framework Directive).
852 European Parliament and Council, 2013. Directive 2013/39/EU of 12 August 2013 amending Directives 2000/60/EC and
853   2008/105/EC as regards priority substances in the field of water policy.
854 Falcieri, F.M., Benetazzo, A., Sclavo, M., Russo, A., Carniel, S., 2014. Po River plume pattern variability investigated
855   from model data. Oceanogr. Coast. Scales, 87, 84–95.
856 Gaillardet, J., Viers, J., Dupré, B., 2003. Trace Elements in River Waters A2 - Holland, Heinrich D., In: Turekian, K.K.;
857   Heinrich, D.H.; Karl, K.T. (Eds.), Treatise on Geochemistry, Oxford, pp. 225–272.
858 Godrijan, J., Marić, D., Tomažić, I., Precali, R., Pfannkuchen, M., 2013. Seasonal phytoplankton dynamics in the coastal
859   waters of the north-eastern Adriatic Sea. J. Sea Res., 77, 32–44.
860 Grilli, F., Marini, M., Degobbis, D., Ferrari, C.R., Fornasiero, P., Russo, A., Gismondi, M., Djakovac, T., Precali, R.,
861   Simonetti, R., 2005. Circulation and horizontal fluxes in the northern Adriatic Sea in the period June 1999–July 2002.
862   Part II: Nutrients transport. Sci. Total Environ., 353, 115–125.
863 Grilli, F., Marini, M., Book, J.W., Campanelli, A., Paschini, E., Russo, A., 2013. Flux of nutrients between the middle
864   and southern Adriatic Sea (Gargano-Split section). Mar. Chem., 153, 1–14.
865 Guo, L., Santschi, P.H., Warnken, K.W., 1995. Dynamics of dissolved organic carbon (DOC) in oceanic environments.
866   Limnol. Oceanogr., 40, 1392–403.
867 Harper, D.J., 1991. The distribution of dissolved cadmium, lead and copper in the Bristol Channel and the outer Severn
868   estuary. Mar. Chem., 33, 131–43.
869 Howell, K.A., Achterberg, E.P., Braungardt, C.B., Tappin, A.D., Turner, D.R., Worsfold, P.J., 2003. The determination
870   of trace metals in estuarine and coastal waters using a voltammetric in situ profiling system. Analyst, 128, 734–741.
871 Illuminati, S., Annibaldi, A., Truzzi, C., Finale, C., Scarponi, G., 2013. Square-wave anodic-stripping voltammetric
872   determination of Cd, Pb and Cu in wine: Set-up and optimization of sample pre-treatment and instrumental parameters.
873   Electrochim. Acta, 104, 148–161.
874 Illuminati, S., Annibaldi, A., Truzzi, C., Libani, G., Mantini, C., Scarponi, G., 2015. Determination of water-soluble,
875   acid-extractable and inert fractions of Cd, Pb and Cu in Antarctic aerosol by square wave anodic stripping voltammetry
876   after sequential extraction and microwave digestion. J. Electroanal. Chem., 755, 182–196.
877 Italian Republic President, 2006. Legislative Decree of the Italian Republic President, n. 152 of the 3 April 2006 on
878   Environmental regulations.
879 Italian Republic President, 2015. Legislative Decree of the Italian Republic President, n. 172 of the 13 October 2015 on
880   the implementation of Directive 2013/39 / EU, amending the directives 2000/60 / EC as regards priority substances
881   in the sector of water policy.
882 Jacquot, J.E., Moffett, J.W., 2015. Copper distribution and speciation across the International GEOTRACES Section
883   GA03. Deep Sea Res. Part II, 116, 187–207.
884 Kolb, M., Rach, P., Schaefer, J., Wild, A., 1992. Investigations of oxidative UV photolysis. I. Sample preparation for the
885   voltammetric determination of zinc, cadmium, lead, copper, nickel, and cobalt in waters. Fresenius J. Anal. Chem.
886   342, 341–349.
887 L'Her Roux, L., Le Roux, S., Appriou, P., 1998. Behavior and speciation of metallic species Cu, Cd, Mn and Fe during
888   estuarine mixing. Mar. Pollut. Bull., 36, 56–64.
889 Marini, M., Jones, B.H., Campanelli, A., Grilli, F., Lee, C.M., 2008. Seasonal variability and Po River plume influence
890   on biochemical properties along western Adriatic coast. J. Geophys. Res. Oceans, 113, 1-18.

27

891 Marini, M., Grilli, F., Guarnieri, A., Jones, B.H., Klajic, Z., Pinardi, N., Sanxhaku, M., 2010. Is the southeastern Adriatic
892   Sea coastal trip an eutrophic area? Estuar. Coast. Shelf Sci. 88, 395–406.
893 Martin, J.H., Knauer, G.A., Flegal, A.R., 1980. Cadmium in, natural waters. In: Cadmium in the Environment, Part 1:
894   Ecological Cycling. Nriagu, J. O. (Ed.), New York, pp. 141–145.
895 Martin, J.-M., Dai, M.-H., Cauwet, G., 1995. Significance of colloids in the biogeochemical cycling of organic carbon
896   and trace metals in the Venice Lagoon (Italy). Limnol. Oceanogr., 40, 119–31.
897 Menden-Deuer, S., Lessard, E.J., 2000. Carbon to volume relationships for dinoflagellates, diatoms, and other protist
898   plankton. Limnol. Oceanogr., 45, 569–579.
899 Michel, P., Boutier, B., Chiffoleau, J.F., 2000. Net fluxes of dissolved arsenic, cadmium, copper, zinc, nitrogen and
900   phosphorus from the Gironde Estuary (France): seasonal variations and trends. Estuar. Coast. Shelf Sci., 51, 451–462.
901 Migon, C., Nicolas, E., 1998. Effects of antipollution policy on anthropogenic lead transfers in the Ligurian Sea. Mar.
902   Pollut. Bull., 36, 775–779.
903 Morel, F.M.M., Hudson, R.J.M., 1985. The geobiological cycle of trace elements in aquatic systems: Redfield revisited.
904   In: Chemical Processes in Lakes. Stumm, W. (Ed.), New York, pp. 251–81.
905 Noel, S., Tercier-Waeber, M.L., Lin, L., Buffle, J., Guenat, O., Koudelka-Hep, M., 2006. Integrated microanalytical
906   system for simultaneous voltammetric measurements of free metal ion concentrations in natural waters. Electroanal.,
907   18, 2061–2069.
908 Ollivier, P., Radakovitch, O., Hamelin, B., 2011. Major and trace element partition and fluxes in the Rhone River. Chem.
909   Geol., 285, 15–31.
910 Oursel, B., Garnier, C., Durrieu, G., Mounier, S., Omanovic, D., Lucas, Y., 2013. Dynamics and fates of trace metals
911   chronically input in a Mediterranean coastal zone impacted by a large urban area. Mar. Pollut. Bull., 69, 137–149.
912 Owens, R.E., Balls, P.W., 1997. Dissolved trace metals in the Tay Estuary. Estuar. Coast. Shelf Sci., 44, 421–434.
913 Parthasarathy, N., Pelletier, M., Buffle, J., 1997. Hollow fiber based supported liquid membrane: a novel analytical system
914   for trace metal analysis. Anal. Chim. Acta, 350, 183-195.
915 Parthasarathy, N., Pelletier, M., Tercier-Waeber, M.L., Buffle, J., 2001. On-line coupling of flow through voltammetric
916   microcell to hollow fiber permeation liquid membrane device for subnanomolar trace metal speciation measurements.
917   Electroanal., 13, 1305–1314.
918 Perez, P., Beiras, R., Fernandez, E., 2010. Monitoring copper toxicity in natural phytoplankton assemblages: application
919   of Fast Repetition Rate fluorometry. Ecotoxicol. Environ. Saf., 73, 1292–1303.
920 Pettine, M., Capri, S., Manganelli, M., Patrolecco, L., Puddu, A., Zoppini, A., 2001. The Dynamics of DOM in the
921   Northern Adriatic Sea. Estuar. Coast. Shelf Sci., 52, 471–489.
922 Powell, R.T., Landing, W.M., Bauer, J.E., 1996. Colloidal trace metals, organic carbon and nitrogen in a southeastern
923   U.S. estuary. Mar. Chem., 55, 165–176.
924 Rivera-Duarte, I., Rosen, G., Lapota, D., Chadwick, D.B., Kear-Padilla, L., Zirino, A., 2005. Copper toxicity to larval
925   stages of three marine invertebrates and copper complexation capacity in San Diego Bay, California. Environ. Sci.
926   Technol., 39, 1542–1546.
927 Russo, A., Artegiani, A., 1996. Adriatic Sea hydrography. Sci. Mar., 60, 33–43.
928 Sadiq, M., 1992. Toxic Metal Chemistry in Marine Environments. Marcel Dekker, Inc., New York.
929 Scarponi, G., Capodaglio, G., Toscano, G., Barbante, C., Cescon, P., 1995. Speciation of lead and cadmium in antarctic
930   seawater: comparison with areas subject to different anthropic influence. Microchem. J., 51, 214–230.
931 Scarponi, G., Turetta, C., Capodaglio, G., Toscano, G., Barbante, C., Moret, I., Cescon, P., 1998. Chemometric studies
932   in the Lagoon of Venice, Italy. 1. The environmental quality of water and sediment matrixes. J. Chem. Inf. Comput.
933   Sci., 38, 552–562.
934 Schiltzer, R., 2017. Ocean Data View, http://odv.awi.de.
935 Scientific Committee on Health, Environmental and Emerging Risks (SCHEER), European Commission, 2017. Scientific
936   advice on Guidance Document n.27: Technical guidance for deriving Environmental Quality Standards. European
937   Union.
938 Semeniuk, D.M., Cullen, J.T., Johnson, W.K., Gagnon, K., Ruth, T.J., Maldonado, M.T., 2009. Plankton copper
939   requirements and uptake in the subarctic Northeast Pacific Ocean. Deep-Sea Res. I, 56, 1130–1142.
940 Sunda, W.G., Huntsman, S.A., 1983. Effect of competitive interactions between manganese and copper on cellular
941   manganese and growth in estuarine and oceanic species of the diatom *Thalassiosira*. Limnol. Oceanogr., 28, 924–34.
942 Tankere, S.P.C., Statham, P.J., 1996. Distribution of dissolved Cd, Cu, Ni and Zn in the Adriatic Sea. Mar. Pollut. Bull.,
943   32, 623–630.
944 Tankere, S.P.C., Price, N.B., Statham, P.J., 2000. Mass balance of trace metals in the Adriatic Sea. J. Mar. Syst., 25, 269–
945   286.
946 Tercier, M.-L., Parthasarathy, N., Buffle, J., 1995. Reproducible, reliable and rugged Hg-plated Ir-based microelectrode
947   for in situ measurements in natural waters. Electroanal., 7, 55–63.
948 Tercier, M.-L., Buffle, J., Graziottin, F., 1998. A novel voltammetric in situ profiling system for continuous real-time
949   monitoring of trace elements in natural waters. Electroanal., 10, 355–363.
950 Tercier-Waeber, M.-L., Belmont-Hebert, C., Buffle, J., 1998. Real-time continuous Mn(II) monitoring in lakes using a
951   novel Voltammetric in situ Profiling System. Environ. Sci. Technol., 32, 1515–1521.

952 Tercier-Waeber, M.-L., Buffle, J., Confalonieri, F., Riccardi, G., Sina, A., Graziottin, F., Fiaccabrino, G.C., Koudelka-
953   Hep, M., 1999. Submersible voltammetric probes for in situ real-time trace element measurements in surface water,
954   groundwater and sediment-water interface. Meas. Sci. Technol., 10, 1202–1213.
955 Tercier-Waeber, M.-L., Buffle, J., 2000. Submersible Online Oxygen Removal System Coupled to an in Situ
956   Voltammetric Probe for Trace Element Monitoring in Freshwater. Environ. Sci. Technol., 34, 4018–4024.
957 Tercier-Waeber, M.-L., Buffle, J., Koudelka-Hep, M., Graziottin, F., 2002. Submersible voltammetric probes for real-
958   time continuous monitoring of trace elements in natural aquatic systems. In: Environmental Electrochemistry:
959   Analysis of Trace Element Biogeochemistry. American Chemical Society, Washington DC, pp. 16–39.
960 Tercier-Waeber, M.-L., Confalonieri, F., Riccardi, G., Sina, A., Noel, S., Buffle, J., Graziottin, F., 2005. Multi physical-
961   chemical profiler for real-time in situ monitoring of trace metal speciation and master variables: development,
962   validation and field applications. Mar. Chem., 97, 216–235.
963 Tercier-Waeber, M.-L., Confalonieri, F., Koudelka-Hep, M., Dessureault-Rompre, J., Graziottin, F., Buffle, J., 2008. Gel-
964   integrated voltammetric microsensors and submersible probes as reliable tools for environmental trace metal analysis
965   and speciation. Electroanal., 20, 240–258.
966 Totti, C., Cangini, M., Ferrari, C., Kraus, R., Pompei, M., Pugnetti, A., Romagnoli, T., Vanucci, S., Socal, G., 2005.
967   Phytoplankton size-distribution and community structure in relation to mucilage occurrence in the northern Adriatic
968   Sea. Sci. Total Environ., 353, 204–217.
969 Twining, B.S., Baines, S.B., Bozard, J.B., Vogt, S., Walker, E.A., Nelson, D.M., 2011. Metal quotas of plankton in the
970   equatorial Pacific Ocean. Deep-Sea Res. Part II, 58, 325–341.
971 Verweij, W., Glazewski, R., De Haan, H., 1992. Speciation of copper in relation to its bioavailability. Chem. Speci.
972   Bioavail., 4, 43–51.
973 Vignati, D., Dominik, J., 2003. The role of coarse colloids as a carrier phase for trace metals in riverine systems. Aquat.
974   Sci., 65, 129–142.
975 Waeles, M., Riso, R.D., Maguer, J.F., Le Corre, P., 2004. Distribution and chemical speciation of dissolved cadmium and
976   copper in the Loire estuary and North Biscay continental shelf, France. Estuar. Coast. Shelf Sci., 59, 49–57.
977 Waeles, M., Tanguy, V., Lespes, G., Riso, R.D., 2008. Behaviour of colloidal trace metals (Cu, Pb and Cd) in estuarine
978   waters: An approach using frontal ultrafiltration (UF) and stripping chronopotentiometric methods (SCP). Estuar.
979   Coast. Shelf Sci., 80, 538–544.
980 Waeles, M., Riso, R.D., Cabon, J.-Y., Maguer, J.-F., L'Helguen, S., 2009. Speciation of dissolved copper and cadmium
981   in the Loire estuary and over the North Biscay continental shelf in spring. Estuar. Coast. Shelf Sci., 84, 139–146.
982 Wold, S., 1978. Cross-validatory estimation of the number of components in factor and principal components models.
983   Technometrics, 20, 397-405.
984 Zago, C., Capodaglio, G., Ceradini, S., Ciceri, G., Abelmoschi, L., Soggia, F., Cescon, P., Scarponi, G., 2000. Benthic
985   fluxes of cadmium, lead, copper and nitrogen species in the northern Adriatic Sea in front of the River Po outflow,
986   Italy. Sci. Total Environ., 246, 121–137.
987 Zago, C., Capodaglio, G., Barbante, C., Giani, M., Moret, I., Scarponi, G., Cescon, P., 2002. Heavy metal distribution
988   and speciation in the northern Adriatic Sea. Chem. Ecol., 18, 39–51.
989

Tab. 1. Concentrations of trace metals along the Po River plume, selected Mediterranean rivers and open Mediterranean Sea.

Site	Dissolved and (total) concentrations (nmol L^{-1})			Reference
	Cd	Pb	Cu	
Po plume 2002	0.12 ± 0.04 (0.14 ± 0.05)	0.33 ± 0.21 (0.52 ± 0.35)	5.3 ± 2.5 (7.1 ± 4.6)	This study
Po river				(Tankere et al., 2000)
summer 1994		1.2 ± 0.92	41 ± 20	
winter 1995		1.5 ± 0.48	57 ± 18	
Po river 1991	0.58	0.72	25.7	(Dorten et al., 1991)
European estuaries				
Marche estuaries (Italy)	0.089-0.18 (0.18-0.36)	0.34-0.72 (0.48-9.7)	6.3-31 (7.9-47)	(Annibaldi et al., 2015)
Arno (Italy)	0.89	1.01	27.5	(Dorten et al., 1991)
Krka (Croatia)	0.015 (0.020)	0.03 (0.14)	4.44 (6.51)	(Cindrić et al., 2015)
Aber-Wrac'h (France)	~0 – 0.36 (~0 – 0.44)		6.3 – 9.4 (6.3 – 14)	(L'Her Roux et al., 1998)
Gironde (France)	0.04 – 0.84		2.2 – 20	(Michel et al., 2000)
Loire (France)	0.08 – 0.29		8.0 – 21	(Waeles et al., 2004)
Rhone (France)		0.33	32.7	(Ollivier et al., 2011)
Huveaunne (France)	0.07	0.64	27	(Oursel et al., 2013)
Jarret (France)	0.07	0.37	28	(Oursel et al., 2013)
Ebro (Spain)	1.07	0.75	15.3	(Dorten et al., 1991)
Severn (UK)	0.98 – 3.6	~1.9	63 – 79	(Harper, 1991)
Tay (UK)	0.11	0.65	13	(Owens and Balls, 1997)
Scheldt (Netherlands)	0.03 – 1.35	0.2 – 2.6	8 – 42	(Baeyens et al., 2005)
World average river	0.71	0.38	23	(Gaillardet et al., 2003)
Northern Adriatic Sea 1994	0.083		7.14	(Tankere and Statham, 1996)
Northern Adriatic Sea, 1996			5.4 ± 2.5	(Zago et al., 2002)
Northern Adriatic Sea, 1997			6.4 ± 2.8	(Zago et al., 2002)
Central Adriatic Sea, 2000-2004	0.14 ± 0.06	0.24 ± 0.14	7.1 ± 3.6	(Annibaldi et al., 2009)
Southern Adriatic Sea 1994	0.076		2.95	(Tankere and Statham, 1996)
Ligurian Sea		0.12 ± 0.04		(Migon and Nicolas, 1998)
Mediterranean Sea	0.062		1.7	(Tankere and Statham, 1996)
Worldwide oceans				
Arctic Ocean	~0.4	-	~3.0	(Aparicio-González et al., 2012)
Atlantic Ocean	~0.1	~0.1	~1.5	(Aparicio-González et al., 2012)
Indian Ocean	~0.2	~0.04	~1.5	(Aparicio-González et al., 2012)
Pacific Ocean	~0.3	~0.04	~1.4	(Aparicio-González et al., 2012)
Southern Ocean	~0.6	~0.03	~2.0	(Aparicio-González et al., 2012)

FIGURE CAPTIONS

Fig. 1. Study are and location of the sampling stations from the Po mouth to the open sea.

Fig. 2. Contour plots of temperature, salinity, dissolved oxygen concentration, and oxygen saturation percentage during the 2002-Adriatic Sea cruise. The white dots represent the sampling points. The transect position is plotted in Fig. 1.

Fig. 3. Contour plots of chlorophyll-a and DOC during the 2002-Adriatic cruise. The white dots represent the sampling points. The transect position is plotted in Fig. 1.

Fig. 4. Contour plots of DIN, nitrates, nitrites, ammonium, phosphates, and silicates during the 2002-Adriatic cruise. The white dots represent the sampling points. The transect position is plotted in Fig. 1.

Fig. 5. Horizontal profiles of Cd (a), Pb (b), and Cu (c) speciation during the 2002-Adriatic cruise. The figures report the total concentration (—●—), the dissolved (—◇—) and the dynamic (---◆--) fraction distribution in the water column, for each sampling station. The dark-grey patterned area represents the particulate fraction calculated by subtraction between the total and the dissolved concentrations, while the light-grey filled area represents the non-dynamic, or colloidal, fraction, computed by subtraction between dissolved and dynamic concentrations.

Fig. 6. Vertical profiles of Cd speciation during the 2002-Adriatic cruise. The figure reports the total concentration (—●—), the dissolved (—◇—) and the dynamic (---◆--) fraction distribution in the water column for each sampling station. The dark-grey patterned area represents the particulate fraction calculated by subtraction between the total and the dissolved concentrations, while the light-grey filled area represents the non-dynamic, or colloidal, fraction, computed by subtraction between dissolved and dynamic concentrations. The transparent grey stripes represent the pycnocline zones.

Fig. 7. Vertical profiles of Pb speciation during the 2002-Adriatic cruise. The figure reports the total concentration (—●—), the dissolved (—◇—) and the dynamic (---◆--) fraction distribution in the water column for each sampling station. The dark-grey patterned area represents the particulate fraction calculated by subtraction between the total and the dissolved concentrations, while the light-grey filled area represents the non-dynamic, or colloidal, fraction, computed by subtraction between dissolved and dynamic concentrations. The transparent grey stripes represent the pycnocline zones.

Fig. 8. Vertical profiles of Cu speciation during the 2002-Adriatic cruise. The figure reports the total concentration (—●—), the dissolved (—◇—) and the dynamic (---◆--) fraction distribution in the water column for each sampling station. The dark-grey patterned area represents the particulate fraction calculated by subtraction between the total and the dissolved concentrations, while the light-grey filled area represents the non-dynamic, or colloidal, fraction, computed by subtraction between dissolved and dynamic concentrations. The transparent grey stripes represent the pycnocline zones.

Fig. 9. PCA plots: (a) plot of the loadings of PC1 vs. PC2; (b) plot of the loadings of PC2 vs. PC3; (c) plot of the scores of PC1 vs. PC2; (d) plot of the scores of PC2 vs. PC3. The following abridgements were used for the variables: temperature (T), salinity (S), density (ρ), dissolved oxygen (O_{2diss}), oxygen saturation percentage ($O_2\%$), turbidity (Turb), chlorophyll-a (Chl-a), Coccolithophorid abundances (Cocco_Ab), Coccolithophorid biomass (Cocco_B), Diatom abundances (Diat_Ab), Diatom biomass (Diat_B), Dinoflagellate abundances (Dinof_Ab), Dinoflagellate biomass (Dinof_B), Phytoflagellate abundances (Phytof_Ab), Phytoflagellate biomass (Phytof_B), total phytoplankton abundance (TotPh_Ab), total phytoplankton biomass (TotPh_B). For metal fraction abridgements see the text in Section 2.3. The objects code refers to the sampling station and to the depth.

Fig. 1.

Fig. 2.

Chlorophyll a (µg C L⁻¹)

DOC (µmol C L⁻¹)

Distance from the Po mouth (km)

Depth (m)
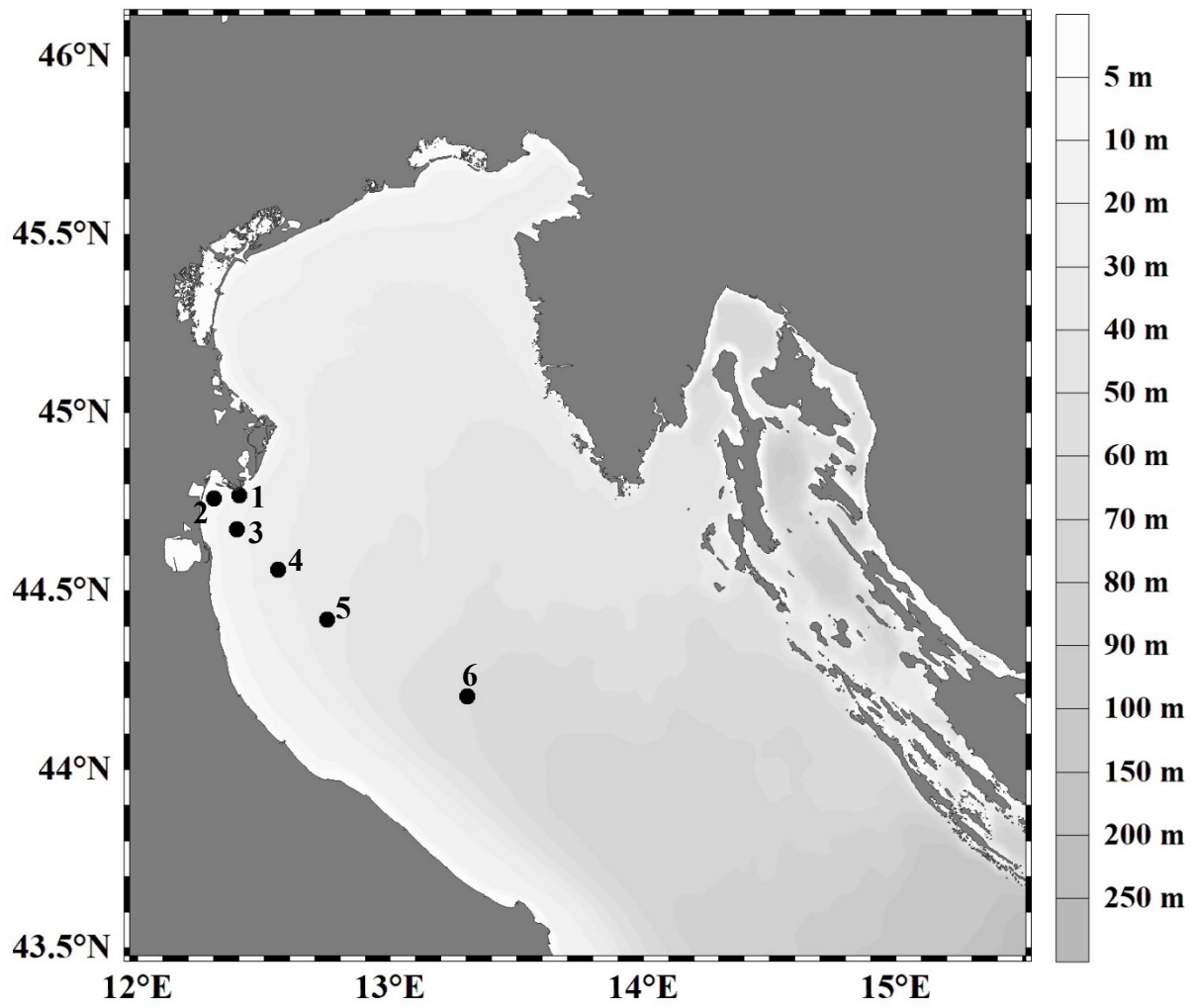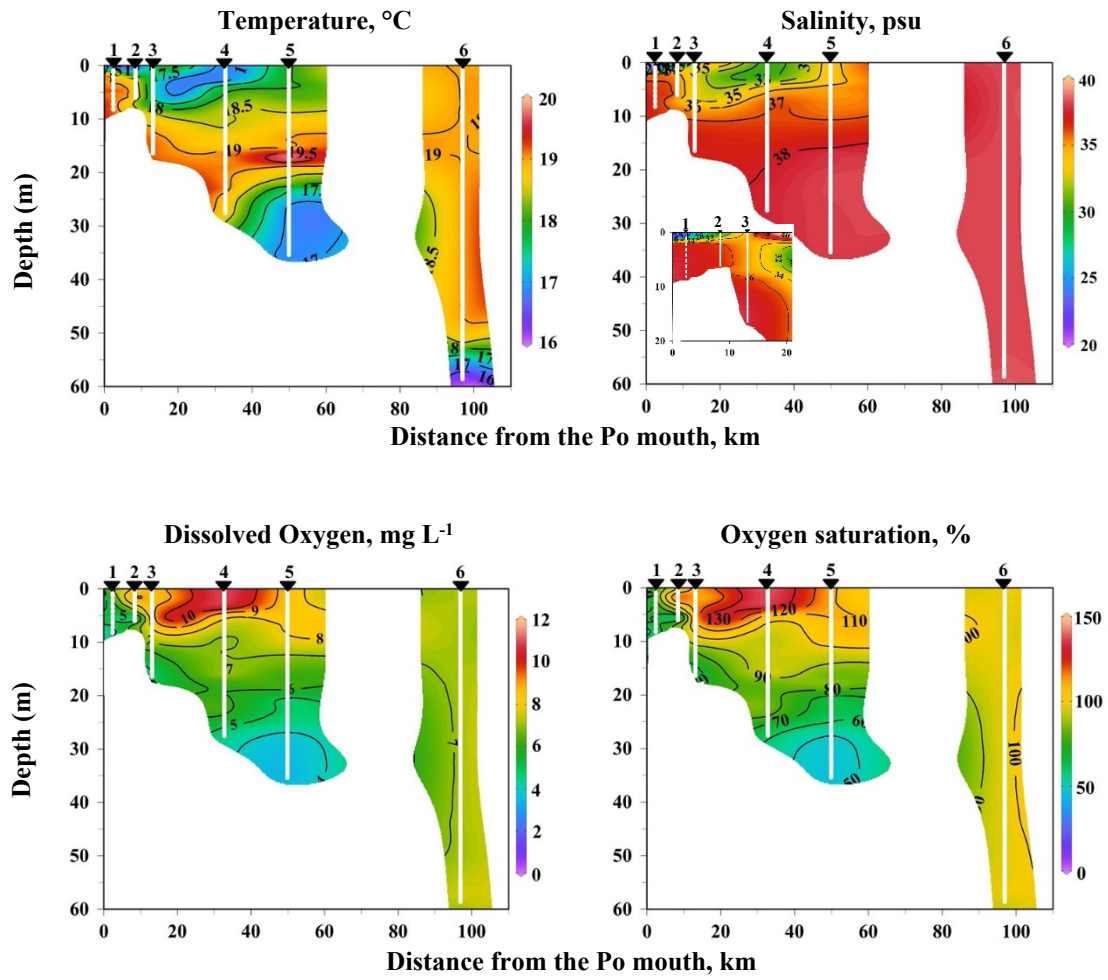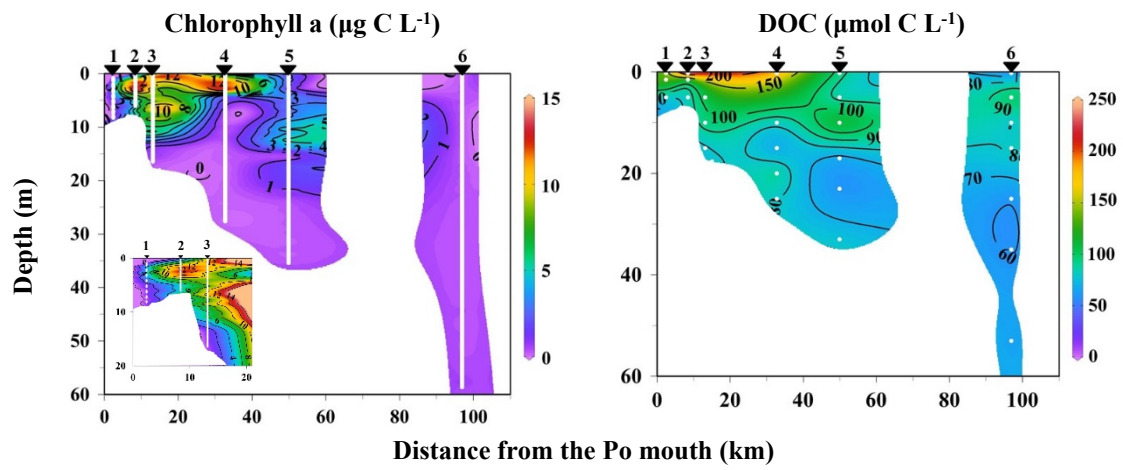
Fig. 3.
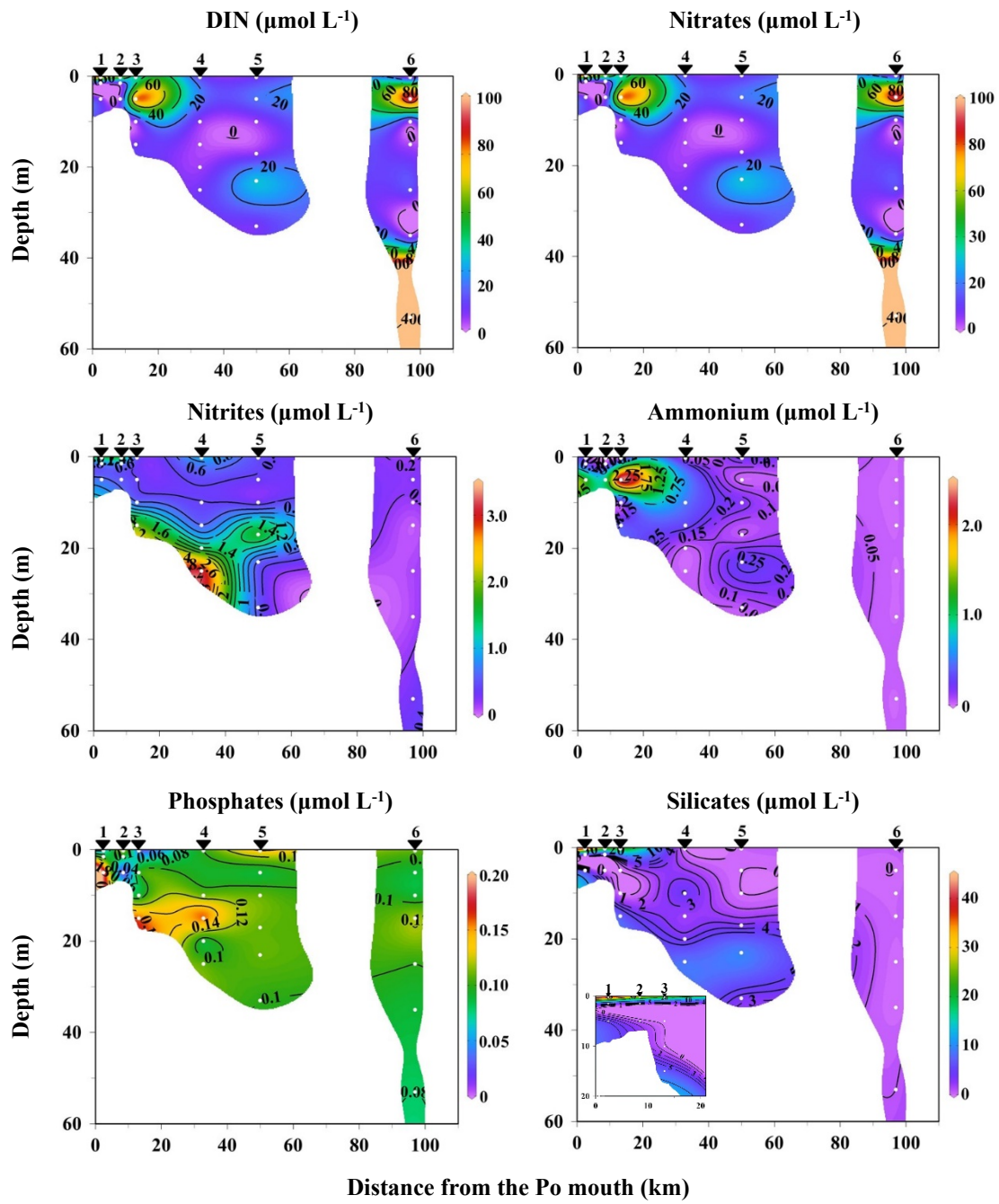
Fig. 4.

Fig. 5.

Cd concentration, nmol L^{-1}

Station 1 | Station 2 | Station 3 | Station 4 | Station 5 | Station 6

Depth, m

Cd$_{tot}$
Cd$_{diss}$
Cd$_{dyn}$
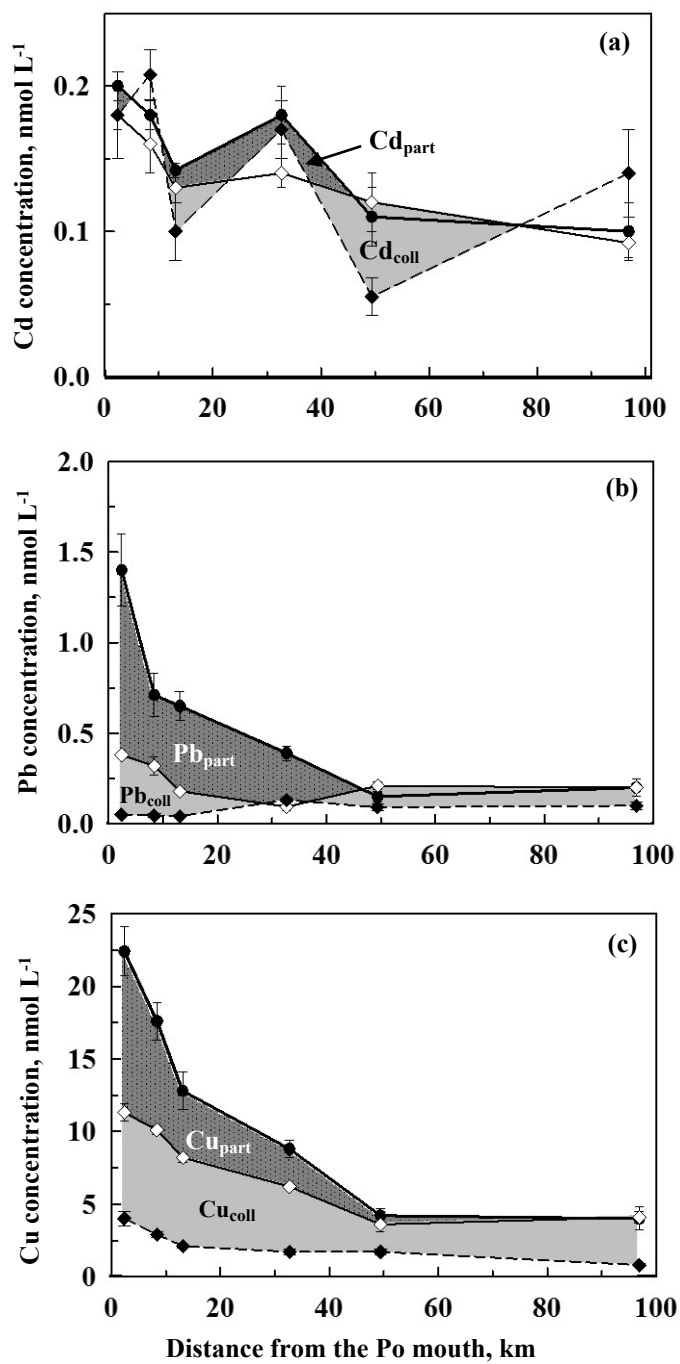
Fig. 6

Pb concentration, nmol L⁻¹
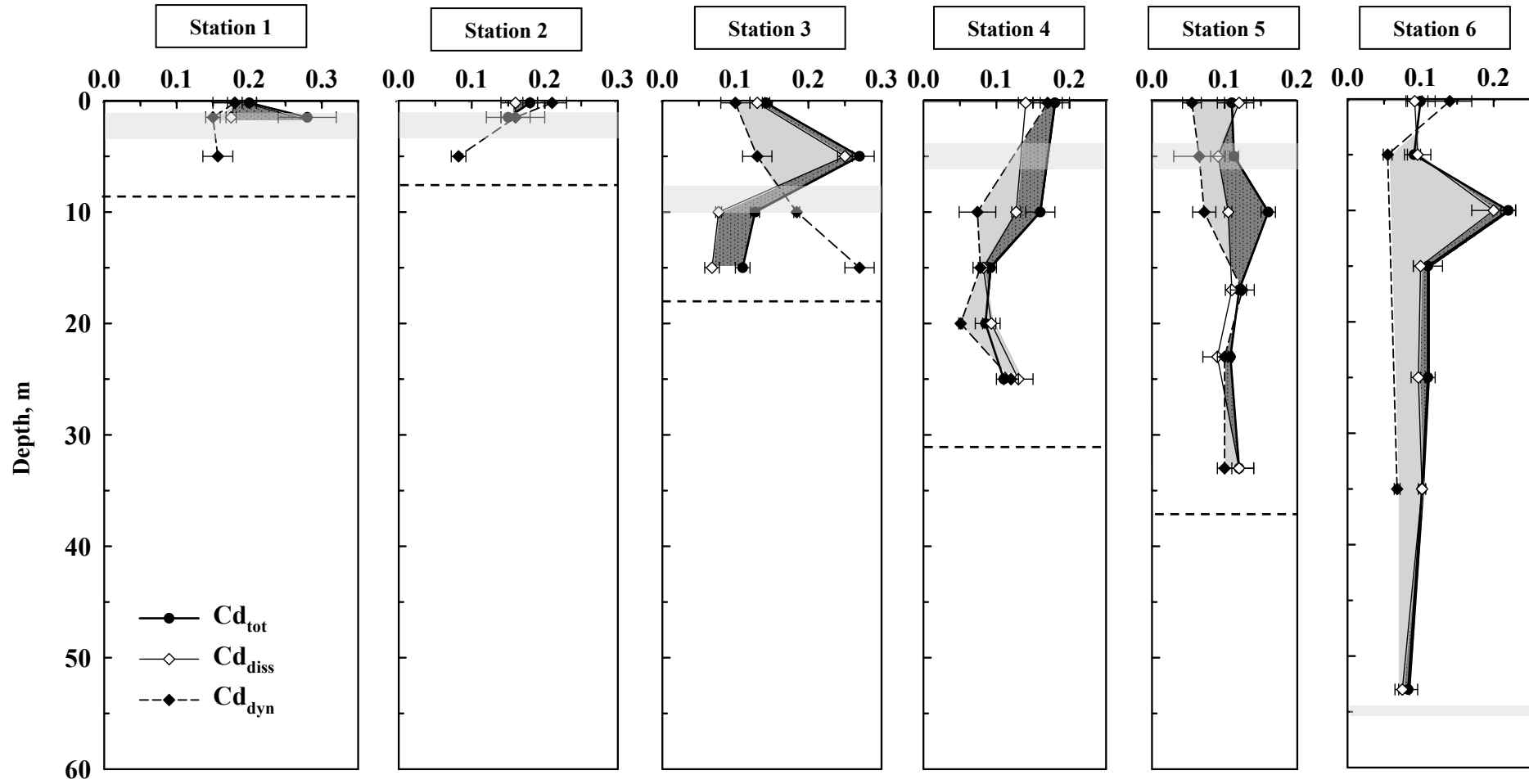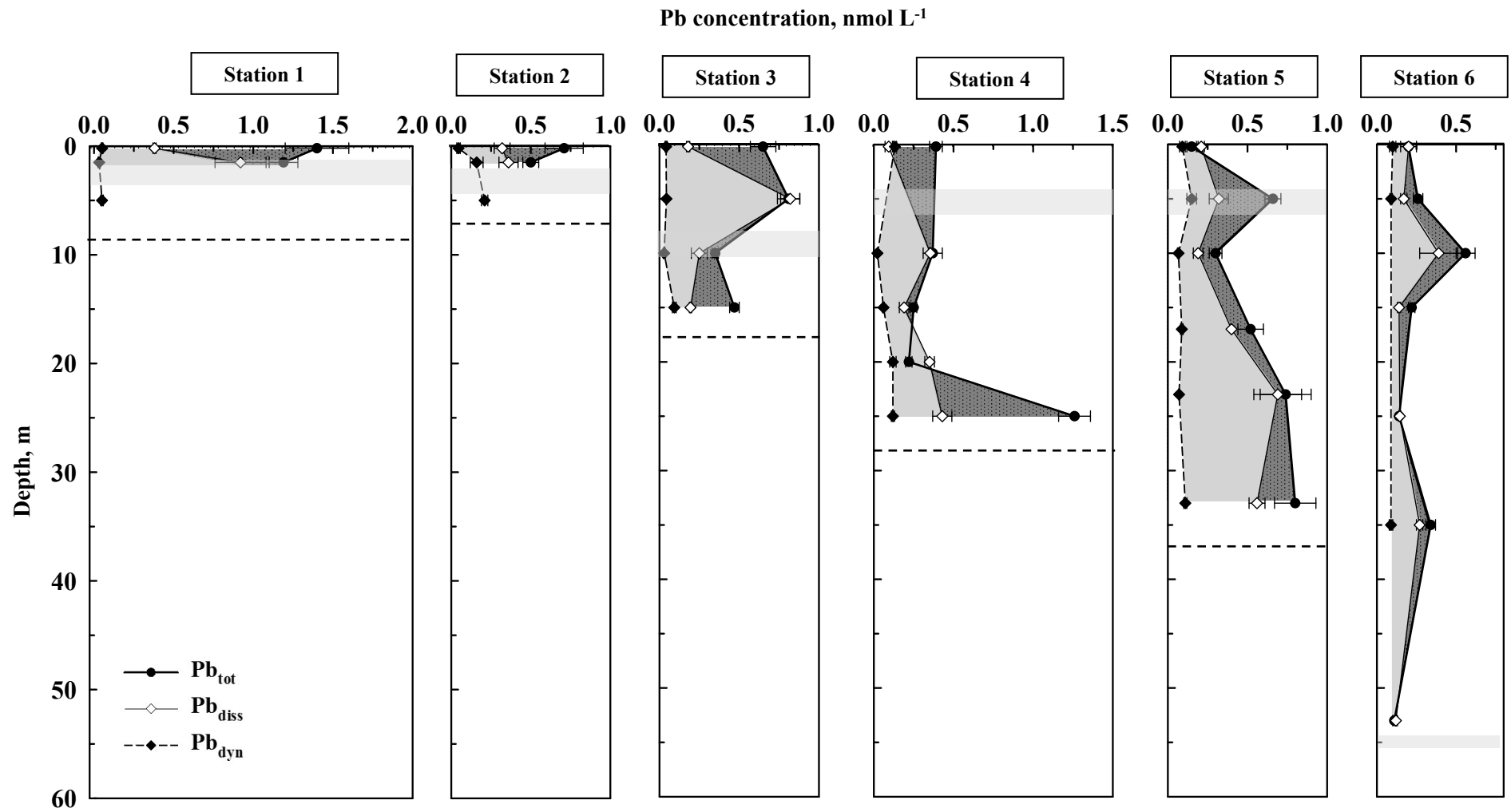
Fig. 7

Cu concentration, nmol L⁻¹
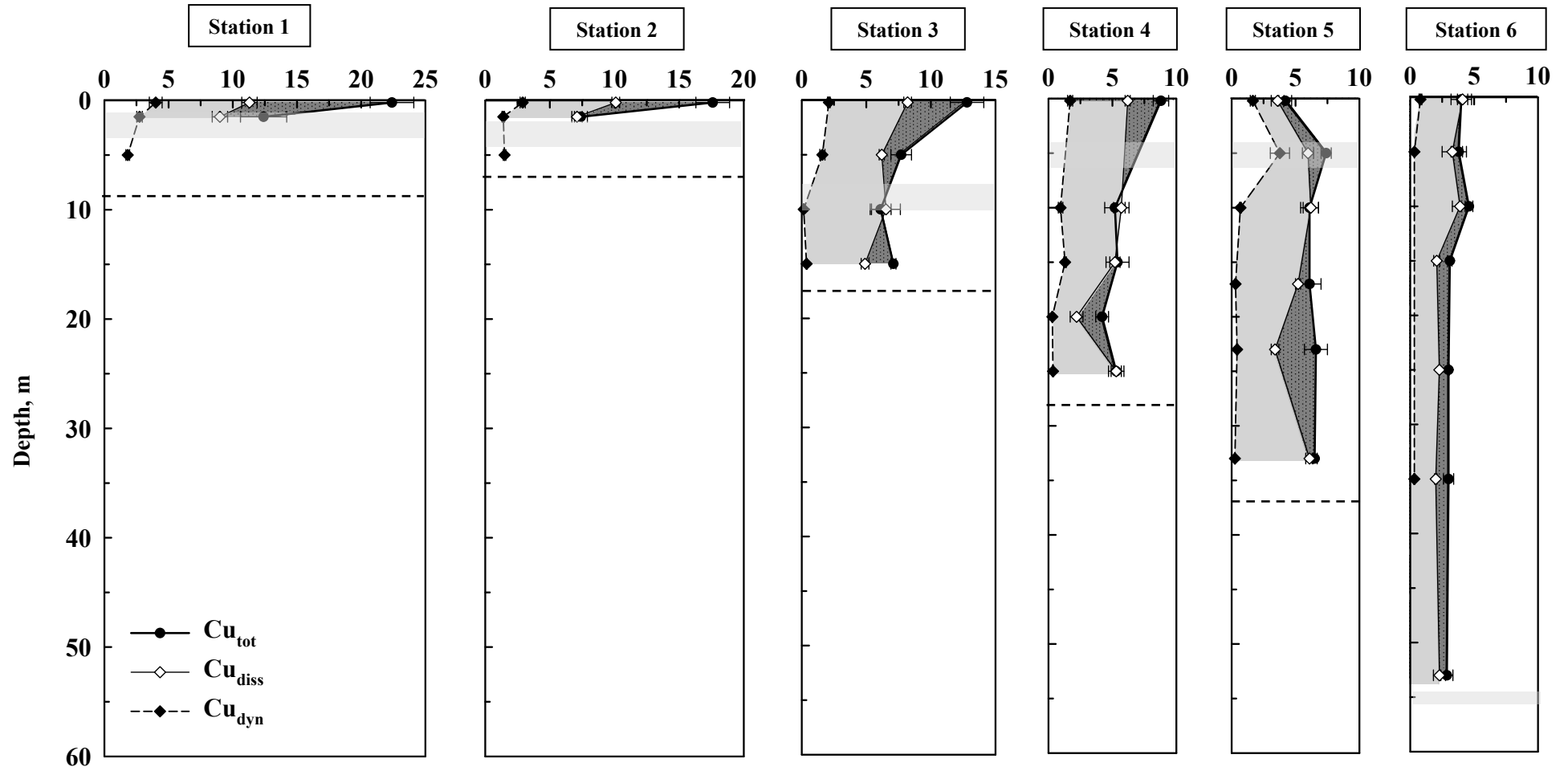
Fig. 8
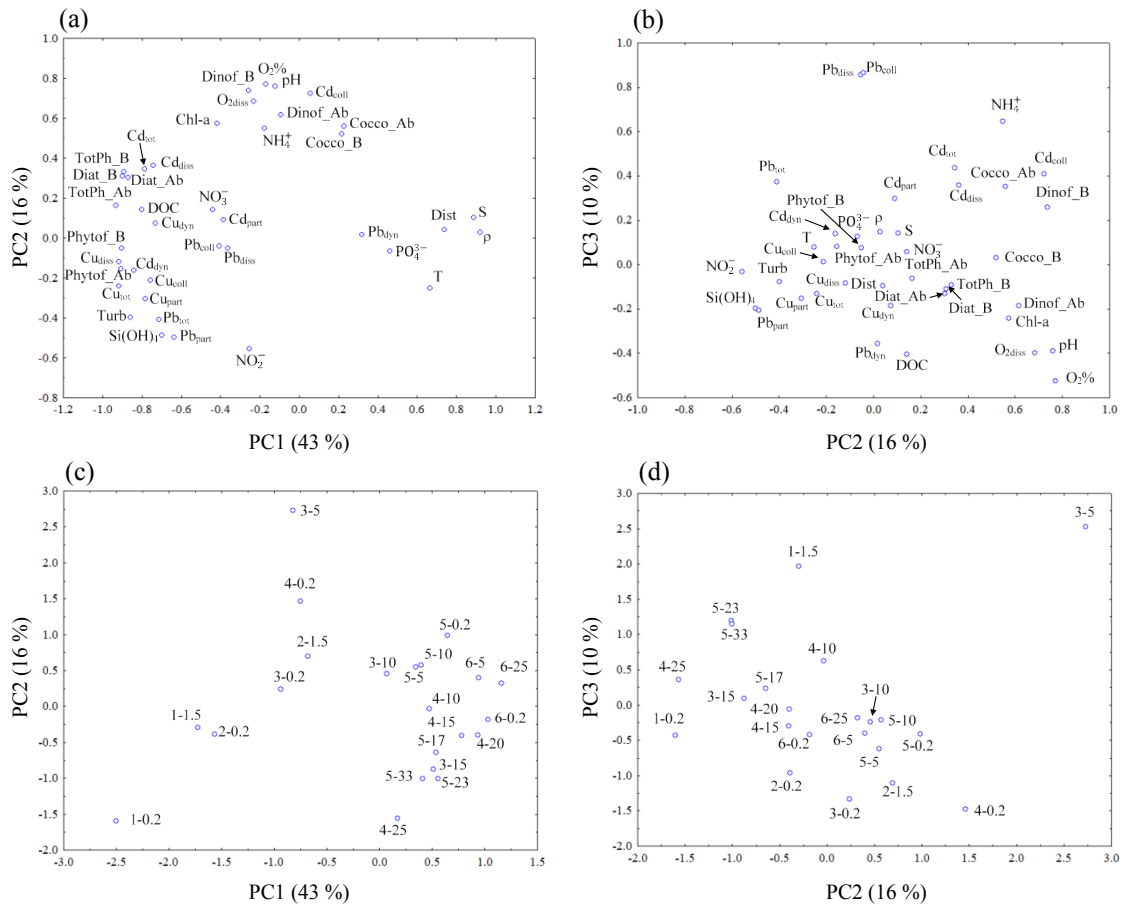
Fig. 9

Supporting information for

In-situ trace metal speciation along the Po River plume (Northern Adriatic Sea) using submersible systems.

Silvia Illuminati*[a], Anna Annibaldi[a], Cristina Truzzi[a], Mary-Lou Tercier-Waeber[b], Stéphane Nöel[b], Jacques Buffle[b], Charlotte B. Braungardt[c], Eric P. Achterberg[d], Kate A. Howell[c,e], David Turner[f], Mauro Marini[g], Tiziana Romagnoli[a], Cecilia Totti[a], Fabio Confalonieri[h], Flavio Graziottin[h], Giuseppe Scarponi[a]

[a]*Department of Life and Environmental Sciences, Polytechnic University of Marche, Italy*
[b]*CABE, Department of Inorganic and Analytical Chemistry, University of Geneva, Switzerland*
[c]*School of Earth, Ocean and Environmental, University of Plymouth, UK*
[d]*National Oceanography Centre, Southampton, School of Ocean and Earth Science, University of Southampton, UK*
[e]*Nanotecture Ltd. Epsilon House, Southampton Science Park, UK*
[f]*Department of Chemistry, University of Göteborg, Sweden*
[g]*Institute of Marine Science, National Research Council (CNR), Ancona, Italy*
[h]*Idronaut Srl, Brugherio (MI), Italy*

*Corresponding Author
e-mail address: s.illuminati@univpm.it

I. 2 Texts
Text S-1. Decontamination procedure
Text S-2. Intercomparison exercises

II. 5 Tables
Table S1. Comparison of the results obtained by the different VIPs available during the cruise for the determination of the Cd, Pb and Cu dynamic fractions.
Table S2. Inter-comparison exercises for the determination of the total fractions and the free ion concentrations of Cd, Pb and Cu.
Table S3. Comparison between the Cd dynamic fraction measured by VIP system and the Cd HCl-extractable dissolved fraction measured by the conventional Metrohm instrumentation.
Table S4. Abundances and biomass of the main phytoplanktonic taxa along the Po river plume.
Table S5. Correlation matrix (Pearson's coefficients) among physical, biological and chemical variables.

III. 1 Figures
Fig. S1. Contour plots of density, pH, and turbidity during the 2002-Adriatic Sea cruise.

Text S-1. Decontamination procedure

The decontamination procedure used for polyethylene bottles, GO-FLO bottles, cellulose mixed ester filters, digester quartz vessels and all other plastic material has already been reported in Annibaldi et al. (2009), Illuminati et al. (2013) and Illuminati et al. (2015). Briefly, careful and prolonged acid washings were applied using, in sequence, detergent solution, 1:10 diluted analytical grade HNO_3, 1:10 diluted superpure HCl and final storage in 1:1000 diluted superpure HCl until use. Similar acid washings were used for sampling equipment (GO-FLO bottle) and filtration apparatus. Membrane filters were cleaned by soaking twice in 1:10 diluted superpure HCl for one week and stored in 1:1000 diluted superpure HCl. Before used GO-FLO bottle, filtration apparatus and membrane filters were three-times washed with ultrapure water and in-situ conditioned with seawater before the contact with samples. As regards the digester quartz vessels, after the above decontamination procedure, these were repeatedly treated with digestion solution (10 mL of 2+1000 diluted ultrapure HCl plus 9 µL of ultrapure H_2O_2) and UV-irradiated for several 12-h cycles.

Text S-2. Inter-comparison exercises

Dynamic fractions. Table S-1 reported the results on the metal dynamic fraction concentrations measured by the six voltammetric probes available on board (below reported as VIP-A from partner Ancona, VIP-B and VIP-C implemented on the MPCP of the Geneva partner; VIP-D and VIP-E from the partner Plymouth and VIP-F from the partner Göteborg). The dynamic inter-comparison here describe is complementary to that in Braungardt et al. (2009), who reported results only for the stations of the study transect closer to the Po river mouth.

Data showed that, excepting for the high values of Cd_{dyn} measured by VIP-A on surface samples, probably due to contamination of the plastic containers in which samples are stored (note that the determination of the metal dynamic content in surface samples was carried out on board because of the inability of the VIPs to be used at depth below to 4 m), a general agreement can be observed between the results obtained for the in-situ measurements of the metal dynamic fractions carried out by all the voltammetric probes, when placed at the same depth.

Total concentrations. Table S-2 reported the results of the total metal concentration, the total HCl-extractable fraction and the *in-situ* total HCl-extractable fraction measured by the GIME-FIA system. Unfortunately, no values of the *in-situ* total acid extractable concentration measured by the GIME-FIA system are available for Stns. 5 and 6 of transect, due to pump rupture. The very few values of the in-situ Cd total HCl-extractable fraction (no GIME-FIA data available for Cd in surface samples) are significantly higher than both the total and the total HCl-extractable concentrations, measured by the conventional Metrohm instrumentations, and which showed similar values, within the experimental error. Concerning Pb, if we exclude the very high values obtained for the first two stations (probably resulting from sample contamination), the other two results available for Stn. 3 and 4 demonstrated that the GIME-FIA procedure allows to determine the "total" lead concentration. On the contrary, for Cu, it can be seen that the total extractable concentration obtained by the GIME-FIA system corresponded to the total acid extractable fraction (a few percent lower) and not to the actual total concentrations. It has to be noted that the GIME-FIA value amounts to about 70% of the total and apparently, this proportion tends to remain almost constant going toward the sea, as well as the acid extractable fraction that always represented ~75% of the total content. Details on the total HCl-extractable variations in the longitudinal profile were reported in Tercier et al. (2005).

Free metal ion concentrations. Data on the free metal ion concentration measured by the CGIME sensor and the HF-PLM technique are very few (Table S-2). The comparison between the two techniques is possible only for Cu. In fact, concerning Pb, only the values given by the HF-PLM are available, while for Cd no signals were obtained from both CGIME sensor and PLM system. Cu_{free} values obtained by the two techniques are very variable; generally, the HF-PLM results are systematically higher than CGIME (Tab. S-2).

Tab. S1. Comparison of the results obtained by the different VIPs available during the cruise for the determination of the Cd, Pb and Cu dynamic fractions. Means (± SD).

Metal	Stn.	Depth, m	Dynamic metal concentration, nmol L^{-1} (±SD)					
			VIP A	VIP B	VIP C	VIP D	VIP E	VIP F
Cd	1	0.2	0.54(±0.01)	0.16	0.19(±0.03)	0.34(±0.05)	−	−
		1.5	0.14(±0.01)	0.21(±0.02)	0.16	−	−	−
		5	0.16	0.18(±0.01)	0.15(±0.02)	−	0.14(±0.03)	−
	2	0.2	0.21	0.22(±0.04)	0.20(±0.0)	−	−	0.21(±0.02)
		1.5	0.15(±0.06)	0.23(±0.03)	0.17	−	−	−
		5	0.08(±0.01)	0.23(±0.02)	0.085(±0.007)	0.08(±0.01)	−	−
	3	0.2	0.40(±0.07)	0.10(±0.02)	0.10(±0.02)	−	0.25(±0.02)	−
		5	−	0.12 ±0.04)	0.13(±0.01)	0.12(±0.02)	0.17	−
		10	0.184(±0.004)	−	−	−	−	−
		15	−	0.26(±0.02)	0.28(±0.01)	−	−	−
	4	0.2	0.17(±0.01)	0.17	0.17(±0.03)	−	−	−
		10	0.07(±0.02)	−	−	−	−	−
		15	0.08(±0.01)	−	−	−	−	−
		20	−	0.053(±0.004)	0.05(±0.0)	−	−	−
		25	−	0.12(±0.02)	0.13(±0.01)	−	−	−
	5	0.2	0.43(±0.09)	0.06(±0.01)	0.14(±0.02)	−	−	−
		4	−	−	−	0.06(±0.04)	0.29(±0.02)	−
		10	0.07(±0.02)	−	−	−	−	−
		18.6	−	0.145(±0.007)	0.12(±0.02)	−	0.125(±0.006)	−
		23	0.10(±0.01)	−	−	−	−	−
		33	−	0.11(±0.01)	0.10(±0.01)	−	−	−
	6	0.2	0.14(±0.03)	0.055(±0.006)	−	−	−	−
		5	−	−	−	−	−	−
		10	−	−	−	−	−	−
		15	−	−	−	−	−	−
		25	0.068(±0.004)	−	−	−	−	−
		35	−	−	−	−	−	−
		53	−	−	−	−	−	−
Pb	1	0.2	0.051(±0.007)	0.23(±0.02)	0.16(±0.02)	−	−	0.051
		1.5	0.032(±0.009)	0.15(±0.02)	0.17(±0.02)	0.034(±0.007)	−	−
		5	0.054(±0.009)	0.11(±0.06)	0.14(±0.06)	0.045(±0.001)	0.12(±0.05)	−
	2	0.2	0.046(±0.011)	0.17(±0.03)	0.24(±0.06)	−	0.30(±0.14)	0.27(±0.07)
		1.5	0.87(±0.11)	0.155(±0.007)	0.183(±0.006)	−	−	−
		5	0.21	0.22(±0.02)	0.185(±0.007)	0.022	0.24	−
	3	0.2	0.042(±0.007)	0.14(±0.01)	0.17(±0.03)	−	−	−
		5	−	0.09(±0.02)	0.10(±0.03)	0.044(±0.002)	0.17(±0.06)	−
		10	0.030(±0.006)	−	−	−	−	−
		15	−	0.09(±0.01)	0.105(±0.007)	−	−	−
	4	0.2	0.13(±0.01)	0.13(±0.02)	0.14(±0.01)	−	−	−
		10	0.024(±0.001)	−	−	−	−	−
		15	0.061(±0.005)	−	−	−	−	−
		20	−	0.14(±0.01)	0.11(±0.0)	−	−	−
		25	−	0.12(±0.006)	0.12(±0.01)	−	−	−
	5	0.2	0.43(±0.09)	0.06(±0.01)	0.14(±0.02)	−	−	−
		4	−	−	−	0.06(±0.04)	0.29(±0.02)	−
		10	0.07(±0.02)	−	−	−	−	−
		18.6	−	0.145(±0.007)	0.12(±0.02)	−	0.125(±0.006)	−
		23	0.10(±0.01)	−	−	−	−	−
		33	−	0.11(±0.01)	0.10(±0.01)	−	−	−
	6	0.2	0.14(±0.03)	0.06(±0.01)	0.14(±0.02)	−	−	−
		5	−	0.055(±0.006)	−	−	−	−
		10	−	−	−	−	−	−
		15	−	−	−	−	−	−
		25	0.068(±0.004)	−	−	−	−	−
		35	−	−	−	−	−	−
		53	−	−	−	−	−	−

Metal	Stn.	Depth, m	Dynamic metal concentration, nmol L^{-1} (±SD)					
			VIP A	VIP B	VIP C	VIP D	VIP E	VIP F
Cu	1	0.2	4.2(±0.20)	3.6(±0.0)	3.4(±0.07)	−	4.6(±0.07)	6.6(±0.92)
		1.5	2.5	2.7(±0.31)	2.7(±0.05)	3.0(±0.10)	−	−
		5	1.8(±0.04)	1.8(±0.18)	1.9(±0.15)	3.6(±0.18)	3.2(±0.83)	−
	2	0.2	2.6(±0.07)	3.1(±0.21)	2.9(±0.15)	−	4.2(±0.50)	7.0(±0.67)
		1.5	1.4(±0.19)	1.4(±0.10)	0.89(±0.06)	−	−	−
		5	0.68(±0.10)	1.5(±0.05)	−	2.7(±0.47)	−	−
	3	0.2	2.1(±0.18)	2.0(±0.12)	2.2(±0.05)	−	−	−
		5	−	0.88(±0.13)	1.6(±0.19)	2.6(±0.06)	1.6(±0.35)	−
		10	0.152(±0.002)	−	−	−	−	−
		15	−	0.40(±0.10)	0.36(±0.02)	−	−	−
	4	0.2	1.6(±0.10)	1.7(±0.21)	2.5(±0.10)	−	−	−
		10	0.95(±0.18)	−	−	−	−	−
		15	1.3(±0.12)	−	−	−	−	−
		20	−	0.34(±0.006)	0.28(±0.006)	−	−	−
		25	−	0.35(±0.05)	0.36(±0.06)	−	−	−
	5	0.2	1.8(±0.21)	1.5(±0.12)	1.6(±0.14)	−	−	−
		5	−	−	−	3.8(±0.75)	−	−
		10	0.69(±0.06)	−	−	3.8	−	−
		18.6	−	0.34(±0.0)	0.30(±0.04)	3.0(±0.68)	−	−
		23	0.43(±0.05)	−	−	−	−	−
		33	−	0.26(±0.02)	0.25(±0.01)	−	−	−
	6	0.2	0.80(±0.11)	−	−	−	−	−
		5	−	0.330(±0.008)	−	−	−	−
		10	−	−	3.0(±0.38)	−	−	−
		15	−	−	−	−	−	−
		25	0.32(±0.04)	−	−	−	−	01.4(±0.11)
		35	−	−	−	−	−	−
		53	−	−	−	−	−	−

Tab. S2. Inter-comparison exercises for the determination of the total fractions and of the free ion concentrations of Cd, Pb and Cu. Means (± SD).

Metal	Stn.	Depth, m	Total metal fractions, nmol L^{-1}			Free metal ion conc, nmol L^{-1}	
			GIME-FIA system	Total	HCl-extractable	CGIME sensor	HF-PLM technique
Cd	1	0.2	–	0.20(±0.01)	0.18(±0.02)	–	–
		1.5	–	0.28(±0.04)	0.27	–	–
		5	0.23	–	–	–	–
	2	0.2	–	0.18(±0.01)	0.14(±0.03)	–	–
		1.5	0.20(±0.05)	0.15(±0.01)	0.15(±0.01)	–	–
		5	0.33(±0.04)	–	–	–	–
	3	0.2	–	0.142(±0.005)	0.13(±0.01)	–	–
		5	–	0.27(±0.02)	0.25(±0.01)	–	–
		10	–	0.13(±0.006)	–	–	–
		15	0.40	0.11(±0.01)	0.09(±0.01)	–	–
	4	0.2	–	0.18(±0.02)	0.13(±0.03)	–	–
		10	–	0.16(±0.02)	–	–	–
		15	–	0.092(±0.008)	–	–	–
		20	0.135(±0.007)	0.08(±0.01)	0.08(±0.02)	–	–
		25	0.29(±0.08)	0.11(±0.01)	0.12(±0.01)	–	–
	5	0.2	–	0.11(±0.02)	0.10(±0.02)	–	–
		5	–	0.113(±0.006)	–	–	–
		10	–	0.16(±0.01)	–	–	–
		18.6	0.26(±0.02)	0.12(±0.01)	–	–	–
		23	–	0.108(±0.003)	–	–	–
		33	–	0.12(±0.02)	–	–	–
	6	0.2	–	0.10(±0.02)	0.084(±0.02)	–	–
		5	–	0.09(±0.01)	–	–	–
		10	–	0.22(±0.01)	–	–	–
		15	–	0.11(±0.02)	–	–	–
		25	–	0.11(±0.01)	–	–	–
		35	–	0.102(±0.001)	–	–	–
		53	–	0.08(±0.01)	–	–	–
Pb	1	0.2	2.0(±0.1)	1.4(±0.2)	1.3(±0.09)	–	–
		1.5	1.4(±0.2)	1.2(±0.09)	0.96	–	0.002
		5	0.94(±0.06)	–	–	–	0.016
	2	0.2	2.5(±0.3)	0.71(±0.12)	0.70(±0.03)	–	0.009
		1.5	2.8(±0.2)	0.50(±0.05)	0.31(±0.05)	–	–
		5	0.84(±0.04)	–	–	–	–
	3	0.2	0.66 (±0.08)	0.65(±0.08)	0.54(±0.05)	–	–
		5	0.70(±0.03)	0.81(±0.07)	0.28(±0.04)	–	0.014
		10	–	0.35(±0.02)	–	–	–
		15	0.80(±0.03)	0.47(±0.03)	0.38(±0.03)	–	0.005
	4	0.2	0.34(±0.04)	0.39(±0.04)	0.33(±0.07)	–	0.010
		10	–	0.37(±0.06)	–	–	–
		15	–	0.25(±0.02)	–	–	–
		20	0.56(±0.04)	0.22(±0.02)	0.14(±0.02)	–	0.011
		25	0.60(±0.04)	1.3(±0.1)	1.0(±0.07)	–	–
	5	0.2	–	0.15(±0.03)	0.16(±0.05)	–	0.009
		4	–	0.66(±0.05)	–	–	0.016
		10	–	0.30(±0.04)	–	–	0.002
		18.6	0.42(±0.11)	0.52(±0.08)	–	–	0.001
		23	–	0.74(±0.16)	–	–	0.001
		33	–	0.80(±0.13)	–	–	–

(to be continued)

(continuing)

Metal	Stn.	Depth, m	Total metal fractions, nmol L^{-1}			Free metal ion conc, nmol L^{-1}	
			GIME-FIA System	Total	HCl-extractable	CGIME sensor	HF-PLM technique
Pb	6	0.2	–	0.20(±0.05)	0.19(±0.05)	–	–
		5	–	0.26(±0.03)	–	–	–
		10	–	0.56(±0.06)	–	–	–
		15	–	0.22(±0.02)	–	–	0.001
		25	–	0.14(±0.0)	–	–	–
		35	–	0.34(±0.03)	–	–	–
		53	–	0.11(±0.01)	–	–	–
Cu	1	0.2	16.3(±0.2)	22.4(±1.7)	16.6(±1.7)	0.62	0.25
		1.5	6.4(±0.1)	12.4(±1.8)	33.2	0.26	0.29
		5	–	–	–	–	–
	2	0.2	11.4(±0.6)	17.6(±1.3)	12.4(±1.7)	0.06	0.17
		1.5	7.6(±0.5)	7.4(±0.5)	7.2(±0.6)	–	–
		5	6.3(±0.09)	–	–	–	–
	3	0.2	8.5(±1.9)	12.5(±1.3)	9.8(±2.4)	–	–
		5	3.3(±0.4)	7.7(±0.8)	7.4(±0.4)	–	0.13
		10	–	–	–	–	–
		15	3.0(±0.2)	7.1(±0.2)	4.5(±0.4)	0.027	0.31
	4	0.2	6.4(±0.04)	8.8(±0.6)	8.1(±0.3)	–	–
		10	–	5.2(±0.8)	–	–	–
		15	–	5.4(±0.9)	–	–	–
		20	1.3(±0.2)	4.2(±0.5)	2.7(±0.2)	0.12	0.18
		25	1.5(±0.1)	5.3(±0.4)	5.7(±0.4	–	–
	5	0.2	–	4.2(±0.5)	3.4(±0.6)	–	0.24
		4	–	7.4(±0.4)	–	–	0.22
		10	–	6.1(±0.7)	–	–	0.27
		18.6	1.2(±0.01)	6.1(±0.9)	–	–	0.37
		23	–	6.6(±0.9)	–	–	0.30
		33	–	6.5(±0.2)	–	–	–
	6	0.2	–	4.0(±0.9)	2.8(±0.2)	–	–
		5	–	3.8(±0.6)	–	–	–
		10	–	4.6(±0.3)	–	–	–
		15	–	3.1(±0.2)	–	–	0.41
		25	–	3.0(±0.06)	–	–	–
		35	–	3.0(±0.4)	–	–	–
		53	–	2.9(±0.5)	–	0.14	–

Tab. S3. Comparison between the Cd dynamic fraction measured by VIP system and the Cd HCl-extractable dissolved fraction measured by the conventional Metrohm instrumentation. Only surface values. Means (± SD). In bold high Cd dynamic values due to contamination problems.

Stations	Cd concentration, nmol L^{-1} (±SD)	
	dynamic frcation	HCl-extractable dissolved fraction
1	0.18(±0.03)	0.18(±0.01)
2	**0.21(±0.02)**	0.14(±0.03)
3	0.10(±0.02)	0.13(±0.04)
4	**0.17(±0.02)**	0.11(±0.03)
5	0.055(±0.013)	0.095(±0.041)
6	**0.14(±0.04)**	0.079(±0.012)

Tab. S4. Abundances ($\times 10^6$ cells L^{-1}) and biomass (μg C L^{-1}) of the main phytoplanktonic taxa along the Po river plume during the October-November 2002 field campaign.. Data are reported as means $\pm$ 10% SD for all the phytoplankton taxa.

Sampling station and depth (m)	Diatoms Abundance 10^6 cells L^{-1}	Diatoms Biomass μg C L^{-1}	Dinoflagellates Abundance 10^4 cells L^{-1}	Dinoflagellates Biomass μg C L^{-1}	Phytoflagellates Abundance 10^6 cells L^{-1}	Phytoflagellates Biomass μg C L^{-1}	Coccolithophorids Abundance 10^4 cells L^{-1}	Coccolithophorids Biomass μg C L^{-1}	Total Abundance 10^6 cells L^{-1}	Total Biomass μg C L^{-1}
Stn. 1										
0.2	4.0	402	0.088	2.5	3.0	10	0	0	6.9	415
1.5	4.6	378	0.080	9.7	2.8	14	0.04	0.028	8.3	402
5	0.85	42	0.029	0.25	2.1	7.3	0	0	3.0	50
Stn. 2										
0.2	3.7	335	2.6	0.65	2.3	7.9	0	0	6.0	343
1.5	4.8	367	1.8	0.87	1.7	5.9	0.010	0.016	6.6	374
5	4.7	353	0.020	0.20	1.8	6.3	0.88	0.23	6.5	360
Stn. 3										
0.2	2.4	219	0.14	3.6	2.1	9.1	0.010	0.006	4.5	232
5	2.9	296	5.6	26	1.4	6.0	2.8	1.7	4.4	329
10	2.5	240	3.2	19	0.67	2.8	0.12	0.42	3.2	263
15	0.36	44	0.90	0.40	1.5	5.4	0.90	0.58	1.9	51
Stn. 4										
0.2	4.5	396	13	20	1.6	7.0	0.059	0.25	6.2	422
10	0.10	7.6	0.74	0.99	0.69	2.6	0.036	0.070	0.80	11
15	0.031	3.4	0.33	0.20	0.64	2.3	0.033	0.022	0.67	5.8
20	0.018	3.3	2.0	2.7	0.59	2.0	0.085	0.092	0.63	8.1
25	0.014	2.6	0.45	0.094	1.5	5.3	0.010	0.014	1.5	8.0
Stn. 5										
0.2	1.3	126	1.2	4.6	0.62	2.9	0.78	4.0	2.0	138
5	1.0	87	2.3	8.3	0.52	2.7	1.2	2.0	1.6	100
10	1.0	124	3.6	5.5	0.45	2.1	1.2	0.69	1.5	132
17	0.86	90	1.7	2.8	0.49	1.7	0.31	0.092	1.4	94
23	0.27	25	1.1	0.41	0.55	2.0	0.048	0.038	0.83	27
33	0.73	72	1.7	3.6	0.60	2.7	0.59	0.19	1.4	79
Stn. 6										
0.2	0.038	6.9	0.71	0.83	0.45	1.8	0.49	0.26	0.49	9.7
5	0.35	34	3.8	7.5	0.25	1.4	0.64	0.75	0.64	44
10	0.045	12	2.0	2.1	0.47	1.6	0.54	1.3	0.54	16
15	0.064	9.8	0.57	1.1	0.37	1.5	0.46	1.8	0.46	13
25	0.024	4.8	1.6	1.3	0.39	1.8	0.46	2.4	0.46	8.4
35	0.029	6.9	0.93	2.3	0.31	1.2	0.36	1.8	0.36	11
53	0.043	4.5	1.1	1.2	0.28	1.0	0.34	0.92	0.34	6.9

Table S5. Correlation matrix (Pearson's coefficients) among physical, biological and chemical variables. Significant correlation ($p \leq 0.05$) are shown in boldface.

	Dist.	Depth	T	S	ρ	Turbid.	O_2	$\%O_{2sat}$	pH	DOC	NO_3^-	NO_2^-	NH_4^+	DIN	PO_4^{3-}	$Si(OH)_4$	Chl-a	DiatomAb	PhytoflAb	DinoflAb	CoccolitAb
Dist.	1.00																				
Depth	0.27	1.00																			
T	**0.46**	0.34	1.00																		
S	**0.57**	**0.55**	**0.53**	1.00																	
ρ	**0.62**	**0.62**	**0.56**	**0.98**	1.00																
Turbid.	-	-	**-0.42**	**-0.89**	**-0.86**	1.00															
O_2	-	-	-0.19	-0.22	-0.29	-0.01	1.00														
$\%O_{2sat}$	-	-	-0.24	-0.15	-0.24	-0.09	**0.85**	1.00													
pH	-	-	-0.17	0.03	-0.07	-0.19	**0.74**	**0.85**	1.00												
DOC	-0.54	**-0.62**	**-0.67**	**-0.68**	**-0.76**	**0.62**	0.40	**0.43**	**0.42**	1.00											
NO_3^-	-0.05	-0.34	-0.29	-0.48	**-0.44**	**0.42**	0.24	0.10	0.08	0.41	1.00										
NO_2^-	**-0.42**	0.22	0.12	-0.21	-0.21	**0.49**	-0.35	-0.30	-0.19	0.14	-0.04	1.00									
NH_4^+	-0.26	-0.11	-0.15	-0.05	-0.06	-0.07	0.21	0.12	0.31	-0.06	0.36	-0.14	1.00								
DIN	-0.06	-0.33	-0.28	**-0.48**	**-0.44**	**0.43**	0.23	0.10	0.08	0.41	**1.00**	-0.02	0.37	1.00							
PO_4^{3-}	0.13	0.25	0.30	0.38	0.34	-0.41	-0.20	-0.16	-0.11	**-0.44**	-0.37	0.14	0.10	-0.36	1.00						
$Si(OH)_4$	**-0.46**	-0.24	-0.36	**-0.77**	**-0.72**	**0.86**	-0.01	-0.17	-0.18	**0.63**	**0.50**	0.40	-0.13	**0.50**	-0.39	1.00					
Chl-a	**-0.45**	**-0.47**	**-0.47**	-0.17	-0.22	0.08	**0.62**	**0.59**	**0.70**	**0.46**	0.11	-0.19	0.25	0.11	**-0.43**	0.04	1.00				
DiatomAb	**-0.64**	**-0.63**	**-0.70**	**-0.72**	**-0.79**	**0.59**	0.38	**0.43**	0.33	**0.74**	0.27	0.04	0.13	0.26	-0.40	0.35	**0.63**	1.00			
PhytoflAb	**-0.71**	**-0.45**	**-0.47**	**-0.77**	**-0.83**	**0.83**	0.08	0.02	0.03	**0.69**	0.25	0.36	0.08	0.26	-0.33	**0.62**	0.26	**0.76**	1.00		
DinoflAb	0.03	-0.22	-0.36	-0.04	-0.08	-0.16	0.16	**0.58**	**0.51**	0.28	0.13	-0.13	0.20	0.13	-0.04	-0.31	0.27	0.35	-0.08	1.00	
CoccolitAb	0.32	0.13	0.10	0.22	0.23	-0.36	0.25	0.17	0.22	-0.28	0.23	-0.36	**0.60**	0.23	0.09	-0.36	0.06	-0.18	-0.29	0.19	1.00
TotPhytoAb	**-0.71**	**-0.60**	**-0.67**	**-0.78**	**-0.85**	**0.71**	0.30	0.31	0.25	**0.77**	0.28	0.16	0.12	0.28	-0.40	**0.47**	**0.54**	**0.97**	**0.89**	0.23	-0.22
DiatomB	**-0.65**	**-0.64**	**-0.71**	**-0.77**	**-0.83**	**0.63**	0.38	**0.42**	0.33	**0.76**	0.33	0.05	0.18	0.33	-0.41	0.41	**0.61**	**0.99**	**0.76**	0.37	-0.13
PhytoflB	**-0.70**	**-0.48**	**-0.52**	**-0.74**	**-0.80**	**0.78**	0.13	0.10	0.12	**0.72**	0.25	0.28	0.12	0.25	-0.37	**0.57**	0.32	**0.78**	**0.99**	-0.01	-0.24
DinoflB	-0.21	-0.31	-0.30	-0.12	-0.17	-0.08	0.29	**0.45**	**0.47**	0.18	0.25	-0.26	**0.59**	0.25	-0.22	-0.30	0.40	**0.43**	0.09	**0.69**	0.39
CoccoliB	0.21	-0.25	-0.04	0.09	0.08	-0.31	**0.42**	0.34	0.15	-0.16	0.11	-0.30	0.27	0.10	0.23	-0.33	0.02	-0.10	-0.28	0.11	**0.49**
TotPhytoB	**-0.65**	**-0.64**	**-0.70**	**-0.76**	**-0.82**	**0.61**	0.38	**0.43**	0.34	**0.76**	0.33	0.04	0.20	0.33	-0.41	0.39	**0.61**	**0.99**	**0.75**	0.39	-0.11
Cd_{tot}	**-0.57**	**-0.45**	**-0.51**	**-0.61**	**-0.68**	**0.50**	0.24	0.21	0.19	**0.51**	0.32	-0.03	**0.57**	0.32	-0.28	0.24	0.35	**0.74**	**0.73**	0.23	0.17
Cd_{part}	-0.38	-0.26	-0.06	-0.28	-0.36	0.19	-0.03	0.03	0.01	0.21	-0.17	-0.09	0.11	-0.18	-0.02	-0.05	0.01	0.40	**0.50**	0.12	-0.04
Cd_{diss}	**-0.49**	**-0.40**	**-0.59**	**-0.58**	**-0.61**	**0.52**	0.32	0.24	0.24	**0.50**	**0.49**	0.08	**0.63**	**0.49**	-0.34	0.32	**0.44**	**0.67**	**0.62**	0.20	0.21
Cd_{dyn}	**-0.59**	-0.26	**-0.52**	**-0.69**	**-0.70**	**0.77**	0.03	-0.01	-0.07	**0.50**	0.31	0.37	0.16	0.31	-0.34	**0.57**	0.36	**0.75**	**0.77**	-0.01	-0.24
Cd_{coll}	0.08	-0.18	-0.12	0.10	0.08	-0.28	0.37	0.33	0.38	-0.03	0.27	-0.37	**0.73**	0.27	-0.07	-0.33	0.16	-0.02	-0.13	0.30	**0.63**
Pb_{tot}	**-0.54**	0.00	-0.38	**-0.59**	**-0.56**	**0.80**	-0.25	-0.36	-0.36	0.32	0.33	0.52	0.15	0.34	-0.36	**0.60**	0.02	0.41	**0.72**	-0.22	-0.19
Pb_{part}	**-0.43**	-0.11	-0.29	**-0.66**	**-0.60**	**0.87**	-0.12	-0.14	-0.20	**0.48**	0.30	**0.65**	-0.21	0.31	-0.37	**0.76**	0.00	0.33	**0.62**	-0.14	-0.33
Pb_{diss}	-0.36	0.15	-0.24	-0.15	-0.16	0.23	-0.27	-0.42	-0.35	-0.07	0.15	0.07	**0.51**	0.15	-0.14	0.05	0.01	0.25	0.40	-0.18	0.08
Pb_{dyn}	0.30	0.17	0.00	0.28	0.31	-0.24	-0.06	0.13	0.00	-0.24	-0.27	0.15	-0.34	-0.27	0.07	-0.34	0.06	-0.09	-0.29	0.25	0.01
Pb_{coll}	-0.39	0.11	-0.24	-0.19	-0.21	0.26	-0.25	-0.41	-0.32	-0.02	0.18	0.04	**0.54**	0.19	-0.14	0.10	0.00	0.26	**0.44**	-0.18	0.07
Cu_{tot}	**-0.63**	**-0.46**	**-0.57**	**-0.92**	**-0.92**	**0.89**	0.13	0.02	-0.05	**0.78**	**0.50**	0.29	0.00	**0.50**	-0.41	**0.89**	0.20	**0.68**	**0.81**	-0.06	-0.29
Cu_{part}	**-0.48**	-0.36	**-0.45**	**-0.87**	**-0.84**	**0.84**	0.03	-0.05	-0.12	**0.70**	**0.57**	0.29	-0.03	**0.57**	-0.38	**0.92**	0.03	**0.51**	**0.69**	-0.08	-0.25
Cu_{diss}	**-0.71**	**-0.50**	**-0.61**	**-0.82**	**-0.85**	**0.79**	0.22	0.10	0.05	**0.75**	0.32	0.22	0.05	0.32	-0.38	**0.70**	0.36	**0.75**	**0.80**	-0.04	-0.31
Cu_{dyn}	**-0.44**	**-0.65**	**-0.56**	**-0.79**	**-0.81**	**0.64**	**0.45**	0.34	0.11	**0.62**	0.38	0.00	0.06	0.38	-0.32	**0.56**	0.21	**0.60**	**0.63**	-0.02	-0.09
Cu_{coll}	**-0.67**	-0.24	**-0.45**	**-0.58**	**-0.60**	**0.65**	-0.01	-0.09	0.00	**0.61**	0.19	0.30	0.03	0.19	-0.30	**0.57**	0.35	**0.63**	**0.66**	-0.04	-0.37

(to be continued)
(continuing)

	TotPhytoAb	DiatomB	PhytoflB	DinoflB	CoccoliB	TotPhytoB	Cd$_{tot}$	Cd$_{part}$	Cd$_{diss}$	Cd$_{dyn}$	Cd$_{coll}$	Pb$_{tot}$	Pb$_{part}$	Pb$_{diss}$	Pb$_{dyn}$	Pb$_{coll}$	Cu$_{tot}$	Cu$_{part}$	Cu$_{diss}$	Cu$_{dyn}$	Cu$_{coll}$
Dist.																					
Depth																					
T																					
S																					
ρ																					
Turbid.																					
O$_2$																					
%O$_{2sat}$																					
pH																					
DOC																					
NO$_3^-$																					
NO$_2^-$																					
NH$_4^+$																					
DIN																					
PO$_4^{3-}$																					
Si(OH)$_4$																					
Chl-a																					
DiatomAb																					
PhytoflAb																					
DinoflAb																					
CoccolitAb																					
TotPhytoAb	1.00																				
DiatomB	**0.97**	1.00																			
PhytoflB	**0.90**	**0.78**	1.00																		
DinoflB	0.34	**0.48**	0.18	1.00																	
CoccoliB	-0.16	-0.07	-0.22	0.29	1.00																
TotPhytoB	**0.96**	**1.00**	**0.77**	**0.51**	-0.05	1.00															
Cd$_{tot}$	**0.78**	**0.77**	**0.76**	**0.53**	-0.05	**0.78**	1.00														
Cd$_{part}$	**0.46**	0.41	**0.52**	0.36	-0.15	**0.42**	**0.62**	1.00													
Cd$_{diss}$	**0.70**	**0.70**	**0.64**	**0.43**	0.04	**0.71**	**0.86**	0.14	1.00												
Cd$_{dyn}$	**0.79**	**0.74**	**0.72**	0.07	-0.40	**0.73**	**0.66**	0.17	**0.73**	1.00											
Cd$_{coll}$	-0.06	0.01	-0.05	**0.56**	**0.57**	0.04	0.37	-0.03	**0.49**	-0.22	1.00										
Pb$_{tot}$	**0.55**	**0.44**	**0.69**	0.03	-0.27	**0.44**	**0.54**	0.23	**0.56**	**0.76**	-0.15	1.00									
Pb$_{part}$	**0.45**	0.37	**0.58**	-0.15	-0.26	0.36	0.21	0.02	0.28	**0.57**	-0.36	**0.79**	1.00								
Pb$_{diss}$	0.32	0.24	0.39	0.23	-0.09	0.25	**0.61**	0.32	**0.57**	**0.50**	0.24	**0.64**	0.04	1.00							
Pb$_{dyn}$	-0.17	-0.16	-0.29	-0.16	0.14	-0.17	**-0.44**	**-0.46**	-0.23	-0.12	-0.16	-0.16	0.01	-0.25	1.00						
Pb$_{coll}$	0.34	0.27	**0.43**	0.27	-0.12	0.28	**0.66**	0.39	**0.59**	**0.50**	0.25	**0.63**	0.04	**0.99**	-0.40	1.00					
Cu$_{tot}$	**0.76**	**0.73**	**0.78**	0.01	-0.27	**0.71**	**0.57**	0.26	**0.53**	**0.73**	-0.24	**0.67**	**0.71**	0.20	-0.35	0.25	1.00				
Cu$_{part}$	**0.61**	**0.57**	**0.65**	-0.08	-0.22	**0.56**	0.41	0.13	0.41	**0.59**	-0.22	**0.57**	**0.65**	0.14	-0.31	0.18	**0.94**	1.00			
Cu$_{diss}$	**0.81**	**0.78**	**0.79**	0.12	-0.28	**0.77**	**0.67**	0.39	**0.58**	**0.77**	-0.22	**0.66**	**0.65**	0.24	-0.37	0.29	**0.90**	**0.70**	1.00		
Cu$_{dyn}$	**0.64**	**0.62**	**0.64**	0.11	0.16	**0.61**	**0.51**	0.23	**0.49**	**0.48**	0.02	**0.48**	**0.52**	0.14	-0.10	0.16	**0.77**	**0.69**	**0.72**	1.00	
Cu$_{coll}$	**0.67**	**0.65**	**0.64**	0.10	**-0.50**	**0.64**	**0.56**	0.38	**0.45**	**0.72**	-0.32	**0.58**	**0.53**	0.23	**-0.45**	0.29	**0.71**	**0.48**	**0.88**	0.30	1.00

Fig. S1. Contour plots of density, pH, redox potential, and turbidity during the 2002-Adriatic Sea cruise. The white dots represent the sampling points. The transect position is plotted in Fig. 1.
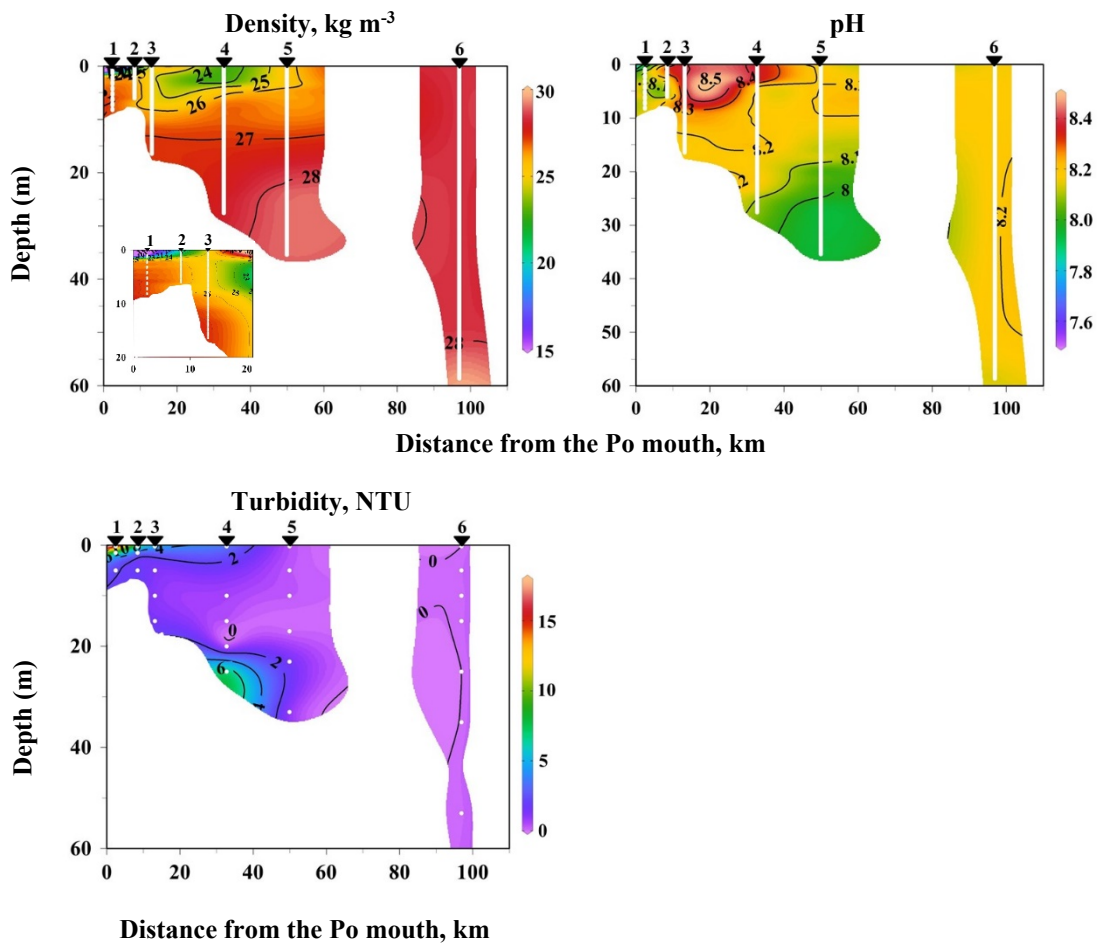
Fig. S1.